

1 **Evidence for pre-climacteric activation of AOX transcription during cold-induced**  
2 **conditioning to ripen in European pear (*Pyrus communis* L.)**

3  
4 Christopher Hendrickson<sup>1</sup>, Seanna Hewitt<sup>1,2</sup>, Mark E. Swanson<sup>3</sup>, Todd Einhorn<sup>4</sup>, and Amit  
5 Dhingra<sup>1,2†</sup>

6  
7 <sup>1</sup>Department of Horticulture, Washington State University, Pullman, WA 99164

8 <sup>2</sup>Molecular Plant Sciences Program, Washington State University, Pullman, WA 99164

9 <sup>3</sup>School of the Environment, Washington State University, Pullman, WA 99164

10 <sup>4</sup>Department of Horticulture, Michigan State University, East Lansing, MI 48824

11  
12 † author to whom correspondence should be addressed: [adhingra@wsu.edu](mailto:adhingra@wsu.edu)

13  
14 **Abstract**

15 European pears (*Pyrus communis* L.) require a range of cold-temperature exposure to induce  
16 ethylene biosynthesis and fruit ripening. Physiological and hormonal responses to cold  
17 temperature storage in pear have been well characterized, but the molecular underpinnings of  
18 these phenomena remain unclear. An established low-temperature conditioning model was used  
19 to induce ripening of ‘D’Anjou’ and ‘Bartlett’ pear cultivars and quantify the expression of key  
20 genes representing ripening-related metabolic pathways in comparison to non-conditioned fruit.  
21 Physiological indicators of pear ripening were recorded, and fruit peel tissue sampled in parallel,  
22 during the cold-conditioning and ripening time-course experiment to correlate gene expression to  
23 ontogeny. Two complementary approaches, Nonparametric Multi-Dimensional Scaling and  
24 efficiency-corrected 2-( $\Delta\Delta Ct$ ), were used to identify genes exhibiting the most variability in  
25 expression. Interestingly, the enhanced alternative oxidase (AOX) transcript abundance at the  
26 pre-climacteric stage in ‘Bartlett’ and ‘D’Anjou’ at the peak of the conditioning treatments  
27 suggests that AOX may play a key and a novel role in the achievement of ripening competency.  
28 There were indications that cold-sensing and signaling elements from ABA and auxin pathways  
29 modulate the S1-S2 ethylene transition in European pears, and that the S1-S2 ethylene  
30 biosynthesis transition is more pronounced in ‘Bartlett’ as compared to ‘D’Anjou’ pear. This  
31 information has implications in preventing post-harvest losses of this important crop.

32  
33 **keywords:** ethylene, System 2 ethylene, ripening, conditioning, AOX

34

## 35 Introduction

36 The fruit is a specialized organ unique to angiosperms that provides a protective environment for  
37 the seeds to develop and mature. In order for the seeds to be disseminated, the fruits undergo a  
38 highly-orchestrated set of physiological and biochemical processes that result in senescence or  
39 ripening [1, 2]. The process of ripening is characterized by the breakdown of chlorophyll and  
40 accumulation of anthocyanins or carotenoids and xanthophylls; the resulting vivid colors make  
41 the fruits visually appealing to potential seed dispersers [3]. The accompanying evolution of  
42 aromatic and volatile compounds, conversion of starches to sugars and softening of the mesocarp  
43 or cortical tissue make the fruits attractive to consumers [4]. The ripening process is categorized  
44 as ‘climacteric’ when there is a respiratory burst along with a peak in ethylene production [5].  
45 All other modes of ripening that do not demonstrate this characteristic behavior are categorized  
46 as ‘non-climacteric.’ While the latter mode of ripening is represented by various fruits such as  
47 citrus, strawberry (*Fragaria × ananassa*), grapes (*Vitis sp.*), etc., the climacteric mode of  
48 ripening is exemplified by bananas (*Musa sp.*), tomato (*Solanum lycopersicum* L.), apple (*Malus*  
49 *x domestica* Borkh.) and pear, to name a few.

50  
51 In climacteric fruit, the biochemistry of ethylene biosynthesis is well understood [6, 7]. As a  
52 result of enhanced auto-stimulatory production of ethylene during respiratory climacteric,  
53 referred to as System 2 ethylene synthesis, the fruit develops a complete profile of desirable  
54 sensory qualities for consumption [8-10]. This is accomplished by the activity of ethylene-  
55 precursor synthesizing and ethylene-synthesizing enzymes, ACC SYNTHASE (ACS) and ACC  
56 OXIDASE (ACO), respectively. In addition to their modulatory effects, these rate-limiting  
57 enzymes are themselves under extensive regulation at the transcriptional, post-transcriptional and  
58 post-translational levels as demonstrated in banana, tomato, etc. [11-14]. Through a combination  
59 of physiological and molecular analyses of climacteric fruit, a comprehensive model of S1 to S2  
60 transition is emerging [5, 15-19] involving numerous phytohormones and molecular signals.

61  
62 Differential abundance of the ABA catabolic gene transcripts ABSCISIC ACID 8’-  
63 HYDROXYLASE 1 and 2 (CYP707A1 and CYP707A2) was shown to correlate with the  
64 upregulation of ACS transcripts and specific developmental stage [20]. These genes inhibit  
65 expression of NCED-like genes in strawberry and tomato, thereby reducing ABA biosynthesis  
66 and promoting cell wall breakdown and ripening [19]. Similar work in peach showed a  
67 correlation between endogenous ABA levels with sensitivity to chilling injury and regulation of  
68 induction of fruit ripening [17, 21]. Auxin is involved in modulating acute and long-term cold  
69 exposure in plants [22, 23]. In climacteric Japanese plum (*Prunus salicina* L.) and melting-flesh  
70 peach (*Prunus persica* L.), development and ripening coincides with prolonged cold temperature  
71 exposure and changes in auxin metabolic processes, indicating that cold responses in fruit tissues  
72 may be influenced in part by intracellular auxin concentrations, though species and cultivars vary  
73 in sensitivity [24, 25]. This, in turn, may be controlled by transport, conjugation, biosynthetic,  
74 and catabolic mechanisms [23]. For example, the ethylene-signaling repressors EIN3 BINDING  
75 FACTOR 1 and 2 were down-regulated in tomato in response to exogenous auxin treatment,  
76 thereby propagating the ethylene signal [26]. Similarly, ACS expression was reported to increase  
77 in banana fruit upon exogenous auxin application [27].

78  
79 In addition to phytohormonal regulation, The MADS-BOX TRANSCRIPTION FACTOR Rin  
80 (MADS-RIN) protein has long-been considered essential for ripening in climacteric fruits, and

81 RIN binding motifs have been identified in the promoter regions of many genes involved in  
82 ethylene biosynthesis and response [28]. Recently, gene-editing based reevaluation of the role of  
83 RIN demonstrated that mutation of this gene results in the production of a protein that actively  
84 inhibits ripening induction [29]. During ripening, the RIN is known to form a transcriptional  
85 regulatory complex that recruits numerous other proteins including specific APETELA 1-like  
86 (AP1-like) and SQUAMOSA PROMOTER BINDING PROTEIN-like (SBP-like) in the  
87 activation of downstream ETHYLENE RESPONSE FACTOR (ERFs), including those leading  
88 to altered ACS or ACO gene expression and protein accumulation [11]. Studies in banana and  
89 tomato have further elucidated the components of this transcriptional activation complex, thereby  
90 adding to the understanding of its function, and the functions of additional MADS-box proteins  
91 in maturing fruits [30, 31]. Recently, the MADS-RIN protein has been implicated in cold-  
92 induced ripening of ‘Bartlett’ pear [32].

93  
94 Several studies in climacteric fruit have suggested that alternative oxidase (AOX) activity affects  
95 ripening through the propagation of a mitochondria-derived signal [33-35]. In mango, the  
96 climacteric stage is facilitated by the up-regulation of cytochrome chain components, and AOX  
97 transcript and protein abundance increase after the climacteric peak, reaching a maximum when  
98 the fruit is ripe [36]. Moreover, stimulation of AOX by exogenous pyruvate enhanced apple  
99 respiration via the alternative respiration pathway at climacteric under cold storage [37]. Similar  
100 observations have been recorded in banana, cucumber, and tomato where cold treatment  
101 enhanced AOX abundance [38-40]. Collectively, these studies demonstrate that AOX is a  
102 product of post-climacteric events and contributes to senescence after the ripening phase.

103 The transition from the autoinhibitory System 1 to autocatalytic System 2 ethylene production  
104 occurs naturally during the developmental course of many fruits such as tomato, apple, peach,  
105 and banana. The postharvest cold treatment has been shown to enhance and synchronize  
106 production of System 2 ethylene in some pome fruits such as ‘Conference’ pear and ‘Golden  
107 Delicious’ and ‘Granny Smith’ apple [41, 42]. Pre- or post-harvest exposure to cold has also  
108 been shown to induce ethylene production, and fruit softening in avocado (*Persea americana*)  
109 and kiwifruit (*Actinidia deliciosa*) [43] [44]. However, in some cultivars of European pear  
110 (*Pyrus communis* L.), a period of exposure to cold temperature after harvest, also called as pre-  
111 ripening period, is required for induction of System 2 ethylene production [45, 46]. Such post-  
112 harvest cold exposure to ripen fruit has been termed ‘conditioning’ [47-49]. Previous studies  
113 have characterized the conditioning needs for different pear cultivars in terms of storage  
114 temperatures, exogenous ethylene exposure and preharvest treatments [47, 48, 50, 51]. In the  
115 absence of exogenous ethylene, conditioning can be achieved by storing the fruit at -1 to 10°C  
116 for 1-15 days for ‘Bartlett’ to 60 days for ‘D’Anjou’ to 90 days for ‘Passe Crassane’ [49]. At the  
117 other end of the spectrum are several Japanese pear (*Pyrus pyrifolia*) cultivars which have no  
118 conditioning requirements and are regarded as non-climacteric. In this context, *Pyrus* displays a  
119 spectrum of fruit phenotypes in terms of response to cold, induction of S2 ethylene, and the onset  
120 of ripening [20]. Interestingly, exogenous application of ethylene can either replace or reduce the  
121 need for conditioning and initiate the ripening climacteric, suggesting the existence of cold-  
122 induced regulatory processes that act independently of the S1-S2 transition [49].

123  
124 While general biochemical pathways involved in ripening of model climacteric fruits are well  
125 studied, more targeted research is necessary to understand cultivar-specific kinetics and  
126 interactions of key ripening-related enzymes in European pears, especially in response to low-

127 temperature conditioning. Previously documented biochemical and genomics data on pear  
128 ripening have revealed a complex regulatory crosstalk between numerous phytohormones,  
129 secondary messengers, signaling pathways, respiration and chromatin modification [5, 11, 32,  
130 52-54]. Differential regulation of these pathways can generate a spectrum of ripening or  
131 postharvest phenotypes, including delayed or accelerated senescent fruit, and fruit with altered  
132 sugar, volatile and nutritional content [15, 55]. Cold-induced physiological responses have been  
133 shown to involve various phytohormones such as abscisic acid (ABA), auxin, jasmonic acid, and  
134 respiration-related signaling [32].

135  
136 Several facets of cold-induced ripening in *Pyrus communis* are becoming clearer. Extensive  
137 studies in fruit and non-fruit crops have identified the presence of C-REPEAT BINDING  
138 FACTOR (CBF)-dependent and independent signaling pathways. A CBF-independent pathway  
139 has been shown to modulate the propagation of the cold-signal in various plant tissues through  
140 the concerted roles of various phytohormone, messenger, and additional elements [56]. It is  
141 expected that phytohormone, respiration and environmental-signaling pathway-targeted analysis  
142 of gene expression across European pear cultivars that differ in their cold requirement may  
143 reveal insights that integrate and regulate the critical transition from S1 to S2 ethylene  
144 production [57, 58].

145  
146 This study was conducted with a focus on expression changes of key genes involved in ripening-  
147 associated biochemical pathways as fruit cultivars representing extreme ends of the chilling  
148 requirement spectrum, ‘Bartlett’ and ‘D’Anjou,’ underwent physiological conditioning by  
149 exposure to predetermined amounts of cold. Nonmetric multidimensional scaling (NMDS) was  
150 used to assess relationships between multiple experimental factors of genotype and physiology  
151 and the associated expression of key genes. NMDS is a multivariate data reduction technique  
152 that identifies axes describing variability among sample units with many measured response  
153 variables [59]. The method condenses the many measured variables in a multivariate data set  
154 into a reduced number of axes that maximize explained variance. Unlike a number of other  
155 methods, however, the method does not require that the measured variables be linear or scaled  
156 similarly. This method was used to accommodate the disparity in a large number of data points  
157 represented by expression values of individual genes, and a relatively lower number of biological  
158 replicates [60]. The NMDS analysis of physiological ripening and expression of target genes  
159 revealed that ‘Bartlett’ and ‘D’Anjou’ fruits follow two dissimilar vectors in response to cold  
160 conditioning, which has implications in preventing post-harvest losses of this important crop.

## 161 162 **Materials and Methods**

### 163 *Physiological conditioning*

164 For this study, fruit was harvested at physiological maturity from two commercial lots in central  
165 Washington state. The fruit was obtained within five days of harvest after temporary storage at  
166 1°C. ‘Bartlett’ fruit had a mean firmness of 76.2 N, and 13.40 °Brix and ‘D’Anjou’ fruit had a  
167 mean firmness of 53.5 N, and 12.66 °Brix at the time of the initiation of the experiment. Pears of  
168 each cultivar were divided into two replicate groups of 1920 fruits each, which were then  
169 maintained at 10°C (Figure 1) for conditioning or 20°C as non-conditioning controls (Sugar and  
170 Einhorn, 2011). After the conditioning period, the fruit was transferred to 180-liter flow-through  
171 respiration chambers held at 20°C for seven days. The flow rate of the chambers was maintained  
172 at 5.0 ml/min with compressed air. The fruit was evaluated for physiological parameters at

173 three-time points: at harvest (i.e., 0% conditioning), 100% conditioning, and 100% ripened,  
 174 which comprised 7 d after completion of conditioning. Peel tissue samples were also collected at  
 175 the stages mentioned above for subsequent comparative gene expression analysis.

176  
 177  
 178

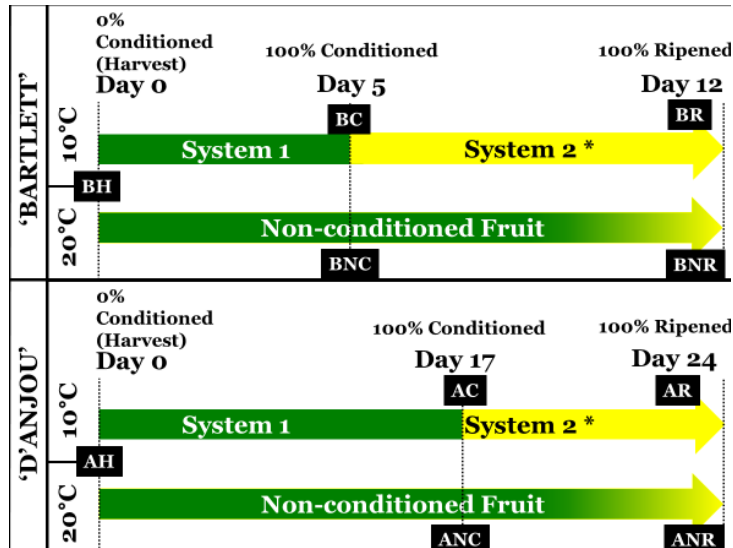


**Figure 1.** Treatment and sampling scheme for 'Bartlett' and 'D'Anjou' fruit. 1,920 fruit of each cultivar were equally distributed. Tissue samples were obtained from Non-Conditioned control fruit maintained at 20°C in parallel to a sampling of fruit that received conditioning treatment. Conditioned fruit was moved to isolated flow-through respiration chambers at 20°C for one week and samples harvested at that time. BH and AH – 'Bartlett' and 'D'Anjou' fruit two days after harvest; BC, AC - 'Bartlett' and 'D'Anjou' fruit at 100% conditioning timepoint; 'BNC, ANC - 'Bartlett' and 'D'Anjou' Non-Conditioned control fruit corresponding to 100% conditioning timepoint for fruit that received conditioning; BR, AR - 'Bartlett' and 'D'Anjou' fruit at 100% Ripened stage; BNR, ANR - 'Bartlett' and 'D'Anjou' Non-Conditioned control fruit corresponding to 100% ripening timepoint for fruit that received conditioning.

179  
 180  
 181  
 182  
 183  
 184  
 185

### *Fruit firmness*

186 Fruit firmness was measured at each sampling time point, and peel tissue samples were collected  
 187 from 10 replicate fruit. Firmness was obtained from two equidistant points around the equatorial  
 188 region of each fruit after removal of the peel with a GS-14 Fruit Texture Analyzer (GÜSS  
 189 Instruments, South Africa) equipped with an 8.0 mm probe set at 5.0 mm flesh penetration. To  
 190 determine significant factors impacting changes in fruit firmness, data were assessed using  
 191 ANOVA, following the statistical approaches described previously [51, 61].

192

### *RNA isolation and cDNA preparation*

194 Peel tissue was obtained from 1 cm wide equatorial region of 3 randomly selected fruit for each  
 195 treatment and flash-frozen in liquid nitrogen. The tissues were then ground using a SPEX  
 196 Freezer/Mill 6870 (Metuchen, NJ USA). Total RNA was extracted from 3 representative time  
 197 points – harvest, fully conditioned fruit maintained at 10°C, and fully ripened fruit derived from  
 198 fruit conditioned at 10°C following the method described previously (Gasic et al., 2004). For  
 199 these time points, corresponding control tissues were also sampled from fruit maintained at 20°C.  
 200 For cDNA preparation, RNA samples were treated with DNaseI to eliminate any DNA  
 201 contamination according to the manufacturer's methods (NEB, Ipswich, MA USA). The RNA  
 202 concentration was determined for each sample using a Nanodrop ND-8000 (ThermoFisher, MA,  
 203 USA). The RNA quality was verified using a denaturing gel and BioAnalyzer 2100 (Agilent, CA  
 204 USA). For each sample, 500 ng of total RNA was used to generate first strand cDNA using the  
 205 Invitrogen VILO kit (Life Technologies, Carlsbad, CA USA). Each cDNA preparation was



206 quantified, and the mean concentration calculated from eight replicate quantification  
207 measurements, recorded using a NanoDrop8000 (Thermo Fisher Scientific, Waltham, MA). The  
208 samples were diluted to a final concentration of 50 ng/uL. Initial qRT-PCR technical replicate  
209 reactions were prepared for each of the 90 selected genes using the iTaq Universal SYBR Green  
210 Supermix (BioRad, Hercules, CA). The genes were selected based on a comprehensive literature  
211 review to represent phytohormone, secondary messenger and environmental signaling pathways  
212 (Supplementary file 3 summarizes the source of literature used to develop the list of genes  
213 involved in S1-S2 ethylene transition and regulation). Reactions were prepared according to the  
214 manufacturer's protocols with 100 ng template cDNA. For the amplification phase, samples were  
215 denatured at 95°C for 2:30 min, followed by 50 cycles of 30 s at 95°C, 30 s at 60°C annealing  
216 temperature and 30 s at 72°C. For the dissociation phase, samples were denatured for one cycle  
217 at 95°C for 30 s, annealed at 60°C for 30 s and denatured gradually to 95°C in increments of  
218 0.5°C to obtain the dissociation curve.

219

#### 220 *Primer design for qRT-PCR*

221 Primers were designed using Primer3 software (<http://frodo.wi.mit.edu/>) using either the doubled  
222 haploid 'Comice' genome [62], or from *Pyrus* ESTs and *Malus × domestica* genome [63] as a  
223 template, and were procured from Sigma–Aldrich (St. Louis, MO). The primers were evaluated  
224 to ensure single amplicon amplification. Amplicons were gel-extracted, sequenced, then  
225 annotated and validated using BLASTX against the NCBI nr database. Primer name, sequences,  
226 target gene, and amplicon sequence, are summarized in Supplementary file 3.

227

#### 228 *Quantitative analysis of targeted gene expression, NMDS analysis*

229 To account for PCR efficiency in the data, Cq values and efficiencies were calculated for each  
230 reaction using the LinRegPCR tool (Ramakers et al., 2003; Ruijter et al., 2009) (Supplementary  
231 file 4). Confidence in Cq values resulting from efficiencies below 1.80 or 2.20 was marked  
232 where appropriate by the gene target in further analyses. The Cq values whose efficiency were  
233 within these bounds, but exceeded (or equaled) 40.00, were deemed unacceptable and identified  
234 in downstream analysis. Similarly, Cq values between (or equal to 35.00-39.99) were marked as  
235 'Low confidence', where appropriate, by the gene target in further analyses.

236

237 Following this, fold-change expression was determined from Cq values of all gene targets  
238 (across all replicates of all samples) between 'D'Anjou' and 'Bartlett' cultivars using the Pfaffl  
239 method (Pfaffl, 2001). Expression of individual genes was normalized in reference to the  
240 geometric mean of *Pyrus communis*  $\beta$ -tubulin and RELATED TO UBIQUITIN1 (RUB1) Cq  
241 values, identified as ideal reference genes with NormFinder (Andersen et al., 2004; Imai et al.,  
242 2014; Vandesompele et al., 2002) (Supplementary file 6). Sequences of these amplicons were  
243 determined using Sanger sequencing, then checked for target amplification using BLASTX  
244 against the NCBI nr database (Supplementary file 3) (Altschul et al., 1990; Gish and States,  
245 1993). This allowed identification of variable expression of individual genes between samples,  
246 following methods reviewed in Rieu and Powers, (2009).

247

248 NMDS: To determine genes contributing the most to variability in the experiment, Cq values for  
249 all remaining gene targets in all biological replicates of all samples were converted into a  
250 community matrix ( $n$  samples by  $p$  genes) for nonmetric multidimensional scaling (NMDS)  
251 using the R package 'Vegan' [64, 65]. The NMDS process assigns rank-order of each gene

252 expression measurement (Cq in this case) across all samples, then depicts variability in a reduced  
253 dimensional space [66]. Graphical or statistical assessment of the grouping of individuals within  
254 treatment groups may then be performed to examine dissimilarity in overall gene expression  
255 within and among treatment groups. In the present study, these group membership factors  
256 included pear cultivar ('Bartlett' and 'D'Anjou'), phenology (harvest, fully conditioned, fully  
257 ripened) and conditioning treatment (conditioned, non-conditioned control). To assess  
258 goodness of fit of the final ordination, a stress coefficient was calculated from the data matrix  
259 (Supplementary file 5).

260  
261 Within the resulting ordination space (NMDS axis 1 x NMDS axis2), the radial distance of  
262 individual gene-associated ordination scores from the origin was calculated and represented as an  
263 assessment of contribution of that gene to variability. Pear cultivar membership appeared to be  
264 strongly related to NMDS axis 1, while phenology (*harvest, conditioned, or ripened*) appeared to  
265 be strongly related to NMDS axis 2 (Supplementary file 10). Sorting radial distance of the  
266 plotted points from the vertex produced a list of genes in order of descending contribution to  
267 variability. Some additional targets were added to the final list of targets for which additional  
268 technical replicates were sought based on *ab initio* and prior unpublished data. From the original  
269 set of 90 selected candidates, genes that had the top 25% of joint biplot lengths (radial distance)  
270 (Supplementary file 7), along with a few additional genes known to be involved in the regulation  
271 of ripening were selected. A total of four replicate reactions were performed for 36 gene targets  
272 in all biological replicates of all samples. A second two-axis NMDS ordination was performed  
273 for 36 targets to visualize variability as a function of each treatment and gene target. A centroid  
274 hull plot was generated from expression data among the unique variety-conditioning-phenology  
275 treatment combinations in RStudio (raw output in Supplementary file 11). Finally, a ray biplot  
276 was generated from 12 ABA, auxin, ethylene, cold-signaling and respiration-related genes  
277 among this final set to indicate relative contributions of pear cultivar and ripeness to the  
278 expression of these highly variable transcripts (raw output in Supplementary file 12).

279  
280 2-delta-delta Ct, Comparative analyses and visualization: Cq values were calculated following  
281 methods described by [67]. In addition to NMDS ordination, fold-change values for individual  
282 genes were analyzed to identify highly variable expression at equivalent stages of fruit  
283 phenology between conditioned and nonconditioned samples. Gene-by-gene comparisons were  
284 conducted after the fold-change data were rendered into a heatmap using a web-accessible tool,  
285 Morpheus (raw output as Supplementary file 13) [68]. In this study, due to the specific  
286 experimental design and limitations of assumptions associated with ANOVA or pairwise t-tests,  
287 differences in expression were visualized using a heatmap, and then ranked in a decreasing order  
288 before being compared with the results of NMDS ordinations. Genes that showed low-  
289 confidence qRT-PCR reaction efficiency or exceeded the parameters described above were  
290 marked on the resulting heatmap with an \*.

291

## 292 **Results and Discussion**

293 In the United States, 97% of the pear orchards exist as low-density plantings with large three-  
294 dimensional trees [69-71]. The tree architecture and orchard organization have a significant  
295 impact on the physiological quality of the fruit [72, 73]. In order to reduce the extent of  
296 variability in fruit quality, fruit used in this study were procured from a commercial warehouse  
297 that had been pre-sorted for size. However, it should be noted, that sorting for size does not

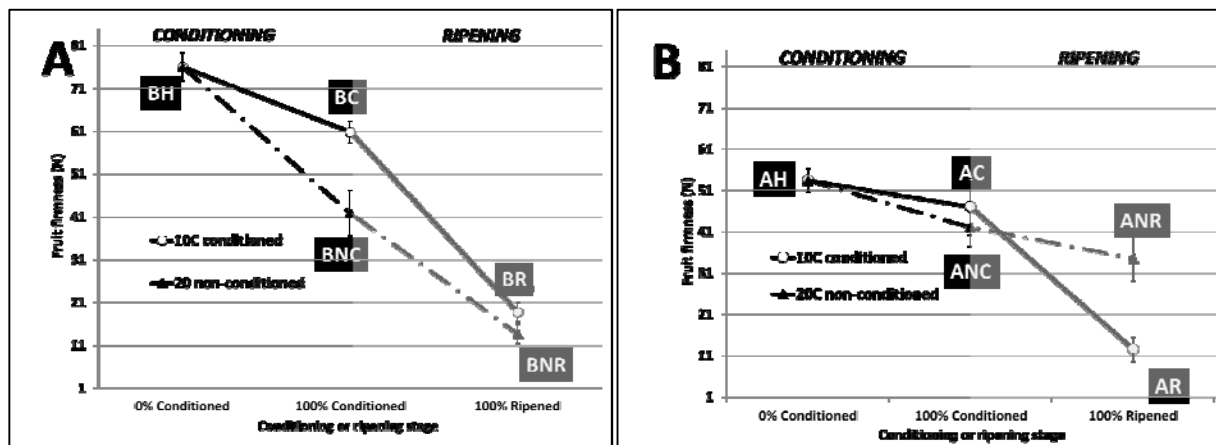
298 necessarily control for variability in the physiological maturity of the fruit, which is affected by  
 299 canopy position [73]. The conditioning treatment provided to fruit resulted in uniform ripening  
 300 as evident from changes in fruit firmness, as demonstrated previously [49].

301

### 302 *Fruit firmness*

303 Cold conditioning of the fruit at 10°C resulted in a reduction of fruit firmness in both ‘Bartlett’  
 304 and ‘D’Anjou’ cultivars as was demonstrated previously [47, 51, 74]. For both cultivars, fruit  
 305 softening accelerated once the fruit was transferred to 20°C. The rate of softening was more  
 306 rapid for ‘Bartlett’ than ‘D’Anjou’ (Figure 2A). Ripening of ‘Bartlett’ requires 15 d of cold  
 307 conditioning, while ‘D’Anjou’ typically requires 60 d of -1°C to attain ripening competency [75,  
 308 76]. The duration of cold conditioning, however, was reduced when conditioning temperatures  
 309 were increased to 10°C (Sugar and Einhorn, 2011). ‘D’Anjou’ pears at advanced physiological  
 310 maturity stages, achieved through delayed harvest, also ripened with markedly shorter  
 311 conditioning periods (Sugar and Einhorn, 2011). The rate of softening showed high variability  
 312 throughout ripening, particularly during the post-conditioning week while the fruit was  
 313 maintained at 20°C (Figure 2, Supplementary file 1). Conversely, fruit that did not receive cold  
 314 conditioning, particularly D’Anjou’ fruit, failed to soften appreciably (Figure 2B).

315



316

317

318 **Figure 2.** Mean fruit firmness (N) through conditioning (white background) and ripening (grey  
 319 background) in A. ‘Bartlett’, and B. ‘D’Anjou’ pear. Fruit was placed into conditioning two days after  
 320 harvest. Error bars represent standard deviation from the mean of measurements recorded from 10  
 321 replicate fruit. Black boxes correspond to fruit treatment sampling stage as follows: BH and AH –  
 322 ‘Bartlett’ and ‘D’Anjou’ fruit two days after harvest; BC, AC - ‘Bartlett’ and ‘D’Anjou’ fruit at 100%  
 323 conditioning timepoint; ‘BNC, ANC - ‘Bartlett’ and ‘D’Anjou’ Non- Conditioned control fruit  
 324 corresponding to 100% conditioning timepoint for fruit that received conditioning; BR, AR - ‘Bartlett’  
 325 and ‘D’Anjou’ fruit at 100% Ripened stage; BNR, ANR - ‘Bartlett’ and ‘D’Anjou’ Non-Conditioned  
 326 control fruit corresponding to 100% ripening timepoint for fruit that received conditioning.

327

### 328 *Quantitative Analysis of Ripening-related Genes and NMDS Analysis*

329 A comprehensive literature review was used to shortlist 90 key ripening-related genes. The genes  
 330 represented phytohormone, secondary messenger, and environmental signaling pathways. The  
 331 expression of these genes was analyzed for both cultivars at different temporal stages during  
 332 conditioning and ripening. A large number of gene targets in comparison with a limited number  
 333 of biological replicates, as in most gene expression studies, presents a key challenge to the



334 dimensionality of the experiment [60]. One methodological solution to this challenge is the use  
335 of data reduction methods such as ordination, in which the information encoded in many  
336 independent variables is distilled into a few dimensions that maximize explained variation  
337 (Wayland, 2003). The NMDS procedure assigns rank-order of the measurement associated with  
338 each unique treatment combination, then depicts variability in a dimensional space that displays  
339 dissimilarity between samples (Kruskal, 1964; Krzywinski and Altman, 2014; Young, 1970).  
340 This approach allows for visualization and pattern recognition among data from numerous  
341 samples, including the potential influence of experimental treatment variables. To assess  
342 goodness of fit of the final ordination, a stress coefficient is calculated from the data matrix,  
343 representing the variability (dissimilarity and dispersion) captured by the set  $n$  dimensions  
344 (Supplementary files 8 and 9).

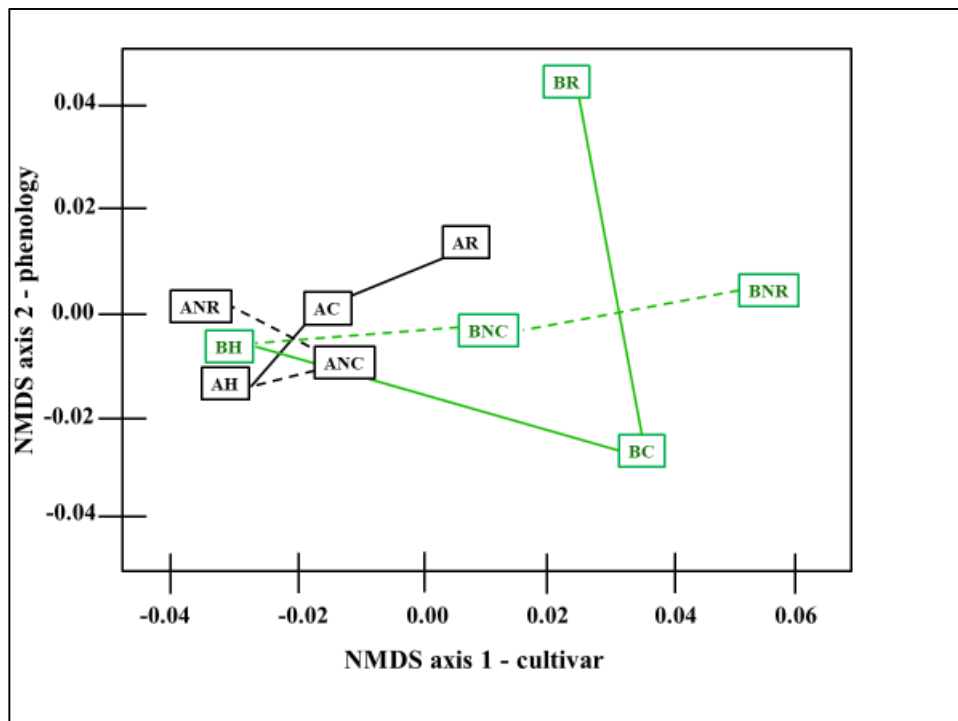
345  
346 The premise of this study, based on non-uniform fruit, warranted a reconsideration of the  
347 statistical tests to be applied to the results and their subsequent interpretation. Recent studies  
348 have suggested for a need to revisit the interpretation of ANOVA, and pairwise  $t$ -tests applied to  
349 biological data, including fruit texture analysis, gene expression and others [77-80]. To provide  
350 physiological context and following protocols applied in prior studies, traditional ANOVA was  
351 utilized to identify significant treatment factors in flesh firmness data [61]. Some of these  
352 reports focus on the identification of differential expression from microarray data, which features  
353 much higher replication than the analytical qRT-PCR data utilized in this study. Indeed, analysis  
354 of qRT-PCR data and identification of significant variance in transcript abundance between  
355 samples remains challenging due to assumptions inherent to traditional ANOVA and  $t$ -tests.  
356 Specifically, these tests assume equal heterogeneity of variance across biological replicates.  
357 Prior reports have demonstrated variable maturation and phenology between fruit depending on  
358 location in the canopy, harvest time, and other factors which would introduce large amounts of  
359 variance in the fruit, and cDNA preparations derived from them [73, 81, 82]. In order to  
360 account for the variability, several methods have been proposed including the TREAT-method  
361 ( $t$ -tests relative to a threshold), which frames p-values derived from  $t$ -tests against an *ab initio*-  
362 derived, biologically meaningful point of significance [78]. More recent responses to these  
363 challenges propose that inclusion of graphical-estimate approaches may complement, or  
364 supplement traditional null-hypothesis based statistical testing, [80]. In this study, nonmetric  
365 multidimensional scaling (NMDS) was used for the visualization of broad trends in fruit  
366 phenology, as well as the contribution of individual genes in the context of cultivar and  
367 treatment.

368  
369 Nonlinear approaches such as those used in the analysis of qRT-PCR expression data have been  
370 used in prior work. Olsvik, Søfteland (83) visualized gene expression with Principal Component  
371 Analysis (PCA), also a nonparametric approach, to identify optimal reference genes from a list of  
372 targets. This enabled rapid, intuitive selection of those targets exhibiting minimum global  
373 variability in the examination of responses in oceanic fish, a heterogeneous environment  
374 imparting high experimental dimensionality. Calculation of this global variability is also used in  
375 the NormFinder tool described above in the initial analysis of qRT-PCR data. Similarly, a  
376 'progress curve' fitting approach has been proposed in which all fluorescence data points of all  
377 reactions are utilized in fitting to the sigmoidal or logistic-growth curve model [84]. NMDS was  
378 selected to assess patterns in gene expression with no assumptions of linearity in the data, similar  
379 scaling of expression values, or other constraints associated with a number of other ordination

380 approaches. The reduction of many dimensions associated with a large number of measured  
381 genes to a much-reduced number of ordination axes allows the efficient exploration of variability  
382 within and among groups.

383  
384 The initial NMDS ordinations achieved stability after 20 iterations, resulting in stress values  
385 ranging from 0.18-0.20 and capturing over 95% of the variability in gene expression data by the  
386 pear cultivar and phenology axes [*NMDS axis 1* (graphically inferred to be associated with  
387 cultivar) and *NMDS axis 2* (graphically inferred to be associated with phenology)]  
388 (Supplementary file 5). This indicated that substantial variability among the expression dataset  
389 was represented by cultivar and conditioning phenology (Figure 3).

390



391  
392

393 **Figure 3.** Geometric treatment group hull centroid plot from final NMDS ordination representing a  
394 grouping of expression data according to pear cultivar, ripeness and conditioning treatment in the two-  
395 dimensional NMDS ordination space of x-axis and y-axis (correlating to cultivar and phenology,  
396 respectively). Dashed lines indicate unconditioned control fruit held at 20°C while solid indicate samples  
397 given conditioning treatment. Black lines indicate 'D'Anjou' while green lines indicate 'Bartlett'. BH  
398 and AH – 'Bartlett' and 'D'Anjou' fruit two days after harvest; BC, AC - 'Bartlett' and 'D'Anjou fruit at  
399 100% conditioning timepoint; 'BNC, ANC - 'Bartlett' and 'D'Anjou' Non- Conditioned control fruit  
400 corresponding to 100% conditioning timepoint for fruit that received conditioning; BR, AR - 'Bartlett'  
401 and 'D'Anjou' fruit at 100% Ripened stage; BNR, ANR - 'Bartlett' and 'D'Anjou' Non-Conditioned  
402 control fruit corresponding to 100% ripening timepoint for fruit that received conditioning. Graph  
403 recreated from raw NMDS output in R with Microsoft PowerPoint. Original R output available in  
404 Supplementary file 11.

405

406 Prior studies have reported a correlation between phenology and the expression of ripening  
407 related genes [54, 85, 86]. However, NMDS analysis provides an approach that can capture  
408 major axes of variance within a multivariate data set, regardless of the scaling of the variables,

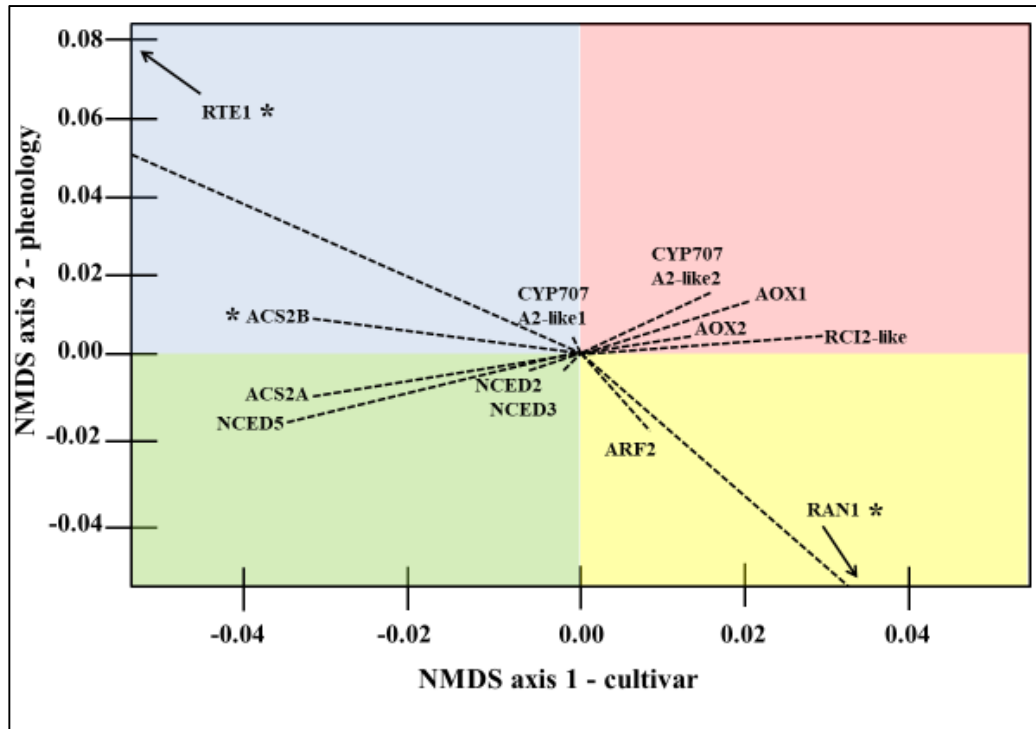
409 and allow for interpretation of the sources of variability. Sorting radial distance of variability in  
410 the expression of genes (according to NMDS axes 1 and 2) revealed numerous phytohormone  
411 and cold-signaling and additional genes in the approximate top third (Supplementary file 10).  
412 Further, expression data sorting revealed a tendency to form clusters by cultivar and treatment  
413 factors. A rightward-shift is seen in ‘Bartlett’-derived expression data in initial and final  
414 ordination spaces, relative to ‘D’Anjou’-derived expression values. Expectedly, unconditioned  
415 controls occupied different regions in the ordination space relative to conditioned fruit of the  
416 same cultivar. While unconditioned ‘Bartlett’ samples remained stationary along the NMDS  
417 axis 1 (cultivar), they grouped to the right of (higher axis 1 score) conditioned fruit.  
418 Alternatively, unconditioned ‘D’Anjou’ samples reverted to the left of (lower axis 1 score)  
419 conditioned samples. Together, this pattern in the ordination space reveals that there is a pre-  
420 existing genotypic variation between ‘Bartlett’ and ‘D’Anjou’ fruit regardless of conditioning  
421 treatments. This information could be used to devise more efficient, cultivar-specific,  
422 conditioning strategies to optimize fruit ripening and quality.

423  
424 Cq values from ripened fruit samples were generally higher on axis 2 (ripeness) of the ordination  
425 space, possibly indicative of the shared physiological responses in the fruit of each cultivar once  
426 they acquired ripening capacity post-conditioning. However, ‘D’Anjou’ fruit exhibit different  
427 overall transcriptional responses compared to ‘Bartlett’ tissues after full conditioning. Of all the  
428 transcripts probed in this work, those from ‘Bartlett’ tissues exhibited a decline in their values on  
429 axis 2 of the ordination space initially, followed by a large increase when the fruit begins to ripen  
430 during the S1-S2 transition. However, ‘D’Anjou’ tissues remain comparatively stable for axis 2  
431 in the ordination space, suggesting underlying differences in conditioning response of this  
432 cultivar as shown in Figure 3. ‘BH’ and ‘AH’ – ‘Bartlett’ and ‘D’Anjou’ fruit at harvest  
433 represents the fruit when the experiments were initiated; BC, AC - ‘Bartlett’ and ‘D’Anjou’ fruit  
434 at 100% conditioning timepoint; ‘BNC, ANC - ‘Bartlett’ and ‘D’Anjou’ Non-Conditioned Fruit  
435 corresponding to 100% conditioning timepoint (see Figure 1); BR, AR - ‘Bartlett’ and ‘D’Anjou’  
436 fruit at 100% Ripened stage; BNR, ANR - ‘Bartlett’ and ‘D’Anjou’ Non-Conditioned Fruit  
437 corresponding to 100% ripening timepoint (see Figure 1). These findings suggest that axis 1 may  
438 be discriminating relative ‘conditioning need’ or ‘propensity for S2-ethylene induction and  
439 ripening’, while axis 2 may discriminate ontogeny of the fruit or relative stage of ethylene  
440 production, or ripening.

441  
442 Data from non-conditioned control samples occupied different regions in the ordination space  
443 and followed a different vector relative to conditioned fruit of the same variety. While non-  
444 conditioned ‘Bartlett’ samples (see BH, BNC, BNR, Figure 3) remained unchanged along the  
445 NMDS axis 1, they grouped to the right of (higher axis 1 score) conditioned and ripened fruit  
446 (see BH, BC, BR, Figure 3). This is consistent with their ripening behavior, where prolonged  
447 storage at 20 °C can soften the fruit, but not necessarily ripen it completely. Alternatively, non-  
448 conditioned ‘D’Anjou’ samples reverted to the left of (lower axis 1 score) conditioned samples  
449 (see AH, ANC, ANR, Figure 3). These patterns in the ordination space illustrate inherent  
450 cultivar-specific differences between ‘Bartlett’ and ‘D’Anjou’ fruit before conditioning  
451 treatments. Overall, this plot helps visualize differential transcript abundance and provides a  
452 basis for understanding how ripening responses manifest in genetically different pear cultivars  
453 subjected to cold conditioning. ‘Bartlett’ pears transitioned from green to yellow as they ripened,  
454 while ‘D’Anjou’ pears generally retained the green peel color.

455  
456  
457  
458  
459  
460  
461  
462  
463  
464

Observed changes in expression of the selected genes in the ordination space, which represent independent variables of phenology, cultivar and treatment, align well with the physiological and molecular models of ripening [15, 24, 45, 54, 85, 87]. Recently, Nham, Macnish (32) identified multiple ABA, auxin, and jasmonic acid-related signaling transcripts as potential putative regulators of cold-induced ripening in European pear, supporting the outcomes of this study. Biplot representation of selected gene vectors and relationship to NMDS ordination axes showed clear grouping according to pear cultivar, correlating calculated radial distance of genes from the vertex of the ordination plot (Figure 4).



465  
466  
467  
468  
469  
470  
471  
472  
473  
474

**Figure 4.** Ray biplot representation of NMDS axis 1 and axis 2 (correlating to cultivar and phenology on the x-axis and y-axis, respectively) contributions to expression variability between select gene targets from final NMDS ordination. Dashed lines represent vector associated with genes in ordination space. Image recreated from raw NMDS output in R. Quadrant shading added to highlight vector separation and is not correlated to, or suggestive of, any physiological state. \*-indicates 'low confidence' values, defined as those from which mean Ct equaled or exceeded 35.00, or whose efficiency exceeded 1.80-2.20 in at least one replicate reactions. Raw R output available in Supplementary file 9.

475  
476  
477  
478  
479  
480  
481  
482

Following the second NMDS ordination of expression data from the final set of selected gene targets, distinct associations between expression patterns of genes with NMDS axes 1 (cultivar) and 2 (phenology) were observed. This indicates that the NMDS approach is an additional avenue to visualize multiple independent variables in a statistically relevant space to identify the most important elements that contribute to variability. This may be especially relevant for RNAseq studies where the number of analyzed genes will always be overwhelmingly higher than the number of biological replicates.

483 The emerging pattern after two rounds of NMDS ordination was that the final third of gene  
484 targets focused on in subsequent 2-( $\Delta\Delta C_t$ )-parametric analysis comprised putative regulatory  
485 control points in the following signaling pathways: cold-perception, abscisic acid signaling,  
486 ethylene signaling, auxin signaling, mitochondrial or peroxisomal metabolite transport, and  
487 respiration-related genes. The expression behavior of selected genes is discussed in the context  
488 of the metabolic pathways they participate in during conditioning and ripening.

489

#### 490 *Cold-perception and ABA signaling*

491 Conditioning temperatures for pear typically range between 0-10°C; this is well within the range  
492 of temperatures at which cold-stress is experienced in any other fruit tissues that do not require  
493 prolonged cold-conditioning to acquire ripening competency [16]. The range of conditioning  
494 requirements of European pear cultivars indicates variation in cold-stress responses, which is  
495 manifest via differential phytohormone and secondary messenger transmission of cold-induced  
496 signals. The data were analyzed to explore how the propagation of cold signals varied between  
497 ‘Bartlett’ and ‘D’Anjou’ tissues. In both Arabidopsis and climacteric fruits, cold acclimation  
498 requires activation of the CBF cold response pathway. ICE1 and HOS1 (INDUCER OF CBF  
499 EXPRESSION 1 and HIGH EXPRESSION OF OSMOTICALLY RESPONSIVE GENES 1,  
500 respectively) comprise initial signaling-elements in cold-perception and initiate the downstream  
501 CBF-pathway [21, 88, 89]. Relatively stable expression of the cold signal inducers across pear  
502 cultivars and in response to conditioning treatments suggests the presence of an alternative cold-  
503 responsive pathway compared to other fruit. Potential candidates could be ABA-signaling or a  
504 prolonged cold-responsive RARE COLD INDUCIBLE (RCI)-pathway specific to pear [90].  
505 Differential expression of the cold-signaling transcription factor HOS1 was not observed, though  
506 it did appear among the genes contributing the most to total variability in expression among the  
507 data. Similarly, analysis of expression from initial technical qRT-PCR replicates did not reveal  
508 much variability in ICE1 or CBF-like expression. This highlights the important insights gained  
509 into gene expression patterns using a spatial reduction approach, compared to an ANOVA-based  
510 comparison of gene expression.

511

512 ABA and auxin-pathways have been implicated in cold-induced signaling [91, 92]. Variation of  
513 transcript abundance from ABA-biosynthetic and signaling genes was observed in this study.  
514 Two pear homologs of ABA-biosynthesis related 9-CIS-EPOXYCAROTENOID  
515 DIOOXYGENASE (NCED)-like genes were found to associate with the left-side of the NMDS-  
516 ordination  $x$ -axis, corresponding to ‘D’Anjou’ fruit. Pear CYTOCHROME P450, FAMILY 707,  
517 SUBFAMILY A POLYPEPTIDE (CYP707A2)-like expression exhibited slightly divergent  
518 orientation in the ordination space. The CYP707A2-vector is extending toward the right of the  
519 NMDS axis 1, indicating an enhanced expression in ‘Bartlett’ throughout the experiment. ABA  
520 accumulation may positively influence the transition towards System 2 ethylene biosynthesis and  
521 ripening, with steady-state levels significantly impacted by NCED-like, and CYP707A2-like  
522 transcript abundance following harvest [20]. A similar impact of ABA accumulation has been  
523 reported in peach, where nearly 900 ABA-related differentially expressed genes were correlated  
524 with variable cold responsive-phenotypes [21]. Analysis of the data in this study suggests that  
525 ABA biosynthetic activity may vary in pear and depend on the conditioning needs of individual  
526 cultivars.

527



528 The NMDS ordination suggests that the ABA-biosynthetic NCED-like gene showed a  
529 correlation with the increased cold requirement in ‘D’Anjou,’ while ABA-catabolic CYP707A2-  
530 like gene was associated with reduced need for cold in ‘Bartlett.’ Increased expression of ABA-  
531 biosynthetic NCED-like genes and reduced expression of ABA-catabolic genes was shown to  
532 correlate with the accumulation of ABA in cold-independent ripening of Asian pear. However,  
533 the expression of these genes remains unclear in cold-dependent ripening of Chinese White pear  
534 (*Pyrus bretschneideri*) [20], and in ‘Braeburn’ apple, which also requires cold-exposure to ripen  
535 [93]. The results in this study show variable transcript abundance of rate-limiting ABA-  
536 biosynthetic genes, providing a critical signature of cultivar-specific cold-response in European  
537 pear exposed to established conditioning protocols (Figure 4). Peak abundance of NCED-like  
538 and ABA-signaling transcripts showed a correlation to the completion of the conditioning  
539 treatment, particularly in ‘D’Anjou.’ At this phenological stage, ‘D’Anjou’ fruit had completed  
540 the conditioning requirement and had attained full ripening competency, which also marked the  
541 induction of S2-associated ACS ethylene biosynthesis (El-Sharkawy, 2004). The correlation  
542 between ABA-pathway transcript vectors in the ordination space share the trends and position  
543 with traditional ethylene-signaling elements, suggesting a collaborative role of these two  
544 pathways in regulating cold-induced S2-induction and ripening in European pear.

#### 545 546 *Ethylene perception and signaling*

547 Cold conditioning initiates the S2 transition in European pear, which activates ethylene  
548 biosynthesis and downstream signaling processes. In this study, the negative and positive  
549 regulators of ethylene-signaling REVERSION-TO-ETHYLENE-SENSITIVITY1 (RTE1) and  
550 RESISTANT-TO-ANTAGONIST1 (RAN1), respectively, exhibited the largest changes in the  
551 biplot vector (Figure 4). The regulatory role of the two genes is evident in the leftward vector  
552 associated with RTE1 expression in the NMDS ordination space (Figure 4). Similarly, a RAN1-  
553 like transcript exhibited a rightward orientation, supporting the proposed role of this gene in  
554 promotion of ethylene signaling, and fruit ripening (Chang et al., 2014; Ma et al. 2012; Qiu et al.,  
555 2012). In Arabidopsis, RAN1 encodes a copper-transporting protein which physically interacts  
556 with the ETHYLENE RECEPTOR 1 (ETR1) to deliver the requisite  $\text{Cu}^{+1}$  ion required for  
557 ethylene sensitivity [94]. RTE1 and RAN1 exhibited notable directionality only in  
558 unconditioned ‘Bartlett,’ unconditioned ‘D’Anjou,’ and fully conditioned ‘D’Anjou’ samples.

559  
560 Further, a large increase in fold-change values was observed only in the unconditioned  
561 ‘D’Anjou’ samples. Upregulation of an RTE1-like gene in unconditioned pear would fit with  
562 observed physiological responses in pear whose conditioning needs are not met; such fruit would  
563 fail to develop ethylene-sensitivity, engage System 2 ethylene biosynthesis or ripen. As a  
564 negative regulator of ethylene-signaling, upregulation of an RTE1 like transcript in  
565 unconditioned ‘D’Anjou’ may indicate a repression mechanism in these fruits. There is some  
566 evidence for a repressive role for this protein in Arabidopsis where *rte1* mutants were able to  
567 restore ethylene sensitivity in the *etr1-2* mutant [95]. In pear, expression of an RTE1-like  
568 transcript appears strongly influenced by the stage of conditioning/ripening and cultivar. The  
569 magnitude change in RAN1 vector indicates its abundance is strongly impacted by cultivar and  
570 phenology, providing the possibility of control of ethylene receptor biogenesis or sensitivity via  
571 access to the required copper ion cofactor. The autocatalytic feedback associated with S2  
572 ethylene may be triggered as a result of this altered receptor activity. The pear qRT-PCR  
573 product showing homology to RAN1 CDS was sequenced, and its identity confirmed using

574 BLAST (Supplementary file 3). A pear RAN homolog was induced at high levels in early  
575 ripening, possibly indicating its role in conferring enhanced ethylene sensitivity to the fruit,  
576 which is a requirement for S2 ethylene production [96]. Characterization of RAN and RTE1-like  
577 homologs in pear may help determine if these genes indeed exhibit regulatory control over the  
578 ripening competency, ethylene signaling or biosynthesis, or cold-signaling.

579  
580 Pear ACS2-like transcripts exhibited vectors near the vertex of the ripeness axis in the biplot but  
581 were located to the left, supporting the role of ACS2 in S1 to S2 transition and ethylene  
582 biosynthesis during conditioning (El-Sharkawy et al., 2004). This narrow transitional period  
583 also appears to coincide with increased RARE COLD-INDUCIBLE (RCI)-like expression. The  
584 role of RCI-like genes is poorly understood outside of a few model systems. In Arabidopsis,  
585 RCI-proteins attenuated ethylene biosynthesis and cold-acclimation by destabilizing ACS  
586 proteins. The 14-3-3 protein RCI1 destabilizes all three ACS types in Arabidopsis [97] via a yet  
587 to be characterized CBF- and ABA-independent cold signaling pathway. This would agree with  
588 the general functional role of 14-3-3 proteins in modulating target protein activity through  
589 physical interaction [98]. Similarly, expression of RCI-like transcripts may be regulated through  
590 a CBF- and ABA-independent pathway of cold-responsive signal transduction [99]. An RCI2-  
591 like transcript oriented toward the right of the NMDS axis 1, in alignment with the recent reports  
592 of its role in the promotion of ripening in tomato (Sivankalyani et al., 2014).

#### 593 594 *Auxin perception and signaling*

595 Changes in free auxin concentrations have been positively correlated to ripening induction in  
596 many other climacteric fruits [5, 15, 26, 57, 100]. In the climacteric Japanese plum, the seasonal  
597 harvest time of fruit was correlated to TIR1-like auxin receptor haplotype [101]. However,  
598 expression of a TRANSPORT INHIBITOR RESPONSE 1 (TIR1)-like auxin receptor did not  
599 vary significantly in this study. While knowledge from other climacteric fruits suggests cold-  
600 adaptive capacity, auxin-sensitivity may be related to specific pear cultivars.

601  
602 Cold-responses in plant tissues may be attenuated from intracellular auxin concentrations, which  
603 in turn may be controlled by transport, conjugation, biosynthetic, and catabolic mechanisms [22].  
604 Recent work in Japanese plum also correlates cold-adaptive capacity to auxin-sensitivity, System  
605 2 ethylene biosynthesis and fruit ripening through a mechanism not yet characterized [101]. The  
606 abundance of some, but not all, auxin-signaling related transcripts displayed variation in this  
607 study. The vector for a transcript bearing homology to an AUXIN-RESPONSE FACTOR 5  
608 (ARF5) oriented toward the right of the cultivar axis (toward 'Bartlett'), but towards reduced  
609 ripeness. This agrees with prior studies where a correlation between ARF-like expression to the  
610 regulation of abscisic acid and ethylene-signaling has been demonstrated (Liu et al., 2013;  
611 Robles et al., 2012; Schaffer et al., 2013; Tacken et al. 2012a). In Arabidopsis, studies have  
612 linked induction of the ARF2 transcriptional activator to ABA, demonstrating the critical  
613 relationship between these two phytohormones in mediating the response to environmental cues.  
614 In tomato, an ARF2-like homolog functions at the intersection between activities of other  
615 phytohormones impacting ethylene, abscisic acid, cytokinins, and salicylic acid signaling [102].

#### 616 617 *Transcription and Respiration Activators*

618 Climacteric fruit is characterized by a concomitant increase in respiration and ethylene  
619 production [46], processes which are expected to be coordinated by various transcriptional

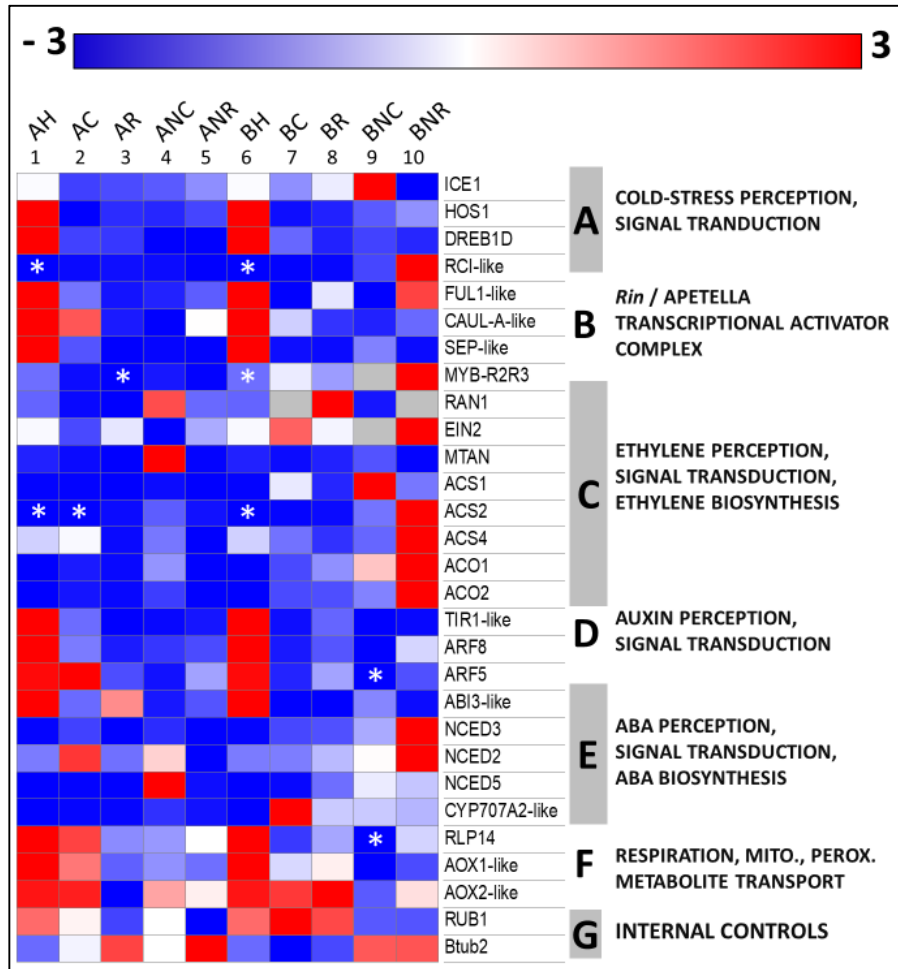
620 activators. Two MADS-box like transcripts were found to be variably expressed between  
621 ‘Bartlett’ and ‘D’Anjou’ fruit that received conditioning treatment and were held at 20°C.  
622 Transcripts bearing homology to the *Malus × domestica* MADS-RIN like transcription factor 8  
623 and 9-like exhibited significant differential expression in response to conditioning and  
624 phenology, but not to the cultivar. This suggests that there may be a shared mechanism between  
625 ‘Bartlett’ and ‘D’Anjou’ during the acquisition of ripening competency that may be mediated by  
626 MADS-box transcriptional regulators. The intricate roles of these important regulatory players  
627 have been detailed extensively in tomato, and research has described the complex network of  
628 interactions and subsequent regulatory influence of the MADS-RIN protein on fruit ripening  
629 induction [28, 103]. MADS-RIN/AP1-like genes play a significant role in tomato ripening and  
630 are thought to recruit the redundant FRUITFUL1 and 2 (FUL1 and 2) MADS-box proteins to  
631 regulate fruit ripening under ethylene-dependent and independent pathways [104, 105].  
632 Conditioned (and not ripened) ‘Bartlett’ and ‘D’Anjou’ samples exhibited far more variability in  
633 expression of both transcriptional activators, suggesting that temporal variation in MADS-box  
634 gene expression results in differential regulation of the S1-S2 transition among pear cultivars. It  
635 seems likely that the expression of this transcription factor may serve as an indicator of pear  
636 ripening competency through conditioning treatments, lending support to the growing  
637 understanding of the MADS-box/AP1/SBP-transcriptional regulatory complex that acts during  
638 the respiratory climacteric.

639  
640 Interestingly, accumulation of ALTERNATIVE OXIDASE (AOX) 1-like transcripts varied  
641 during phenology of ‘Bartlett’ and ‘D’Anjou’ samples. Transcript abundance peaked in the  
642 “100% Conditioned” stage of both cultivars, which is a pre-climacteric stage, as the fruit is yet to  
643 transition to S2 stage [35]. This is intriguing since the expression of AOX has been shown to  
644 coincide with the climacteric peak, a characteristic of climacteric fruit [37, 106]. However,  
645 AOX-1 expression may have peaked between sampling time points, particularly in initial  
646 responses to conditioning environments. These results were not observed for AOX2-like  
647 transcripts, differing from trends previously reported in mango and tomato fruit [34, 107, 108].

648  
649 AOX1 and AOX2-like expression has been reported in many fruit systems, with AOX isoforms  
650 displaying responses to a broad range of stresses, including cold-stress. Knock-down AOX in  
651 tomato delayed ripening, indicating a regulatory role of AOX [109]. Notably, AOX  
652 overexpression tomato lines were shown to be far less responsive to the ethylene signaling  
653 inhibitor 1-methylcyclopropene (1-MCP), while knock-out lines were highly responsive. Thus,  
654 in European pear, respiratory partitioning into the alternative pathway may impact S2 ethylene  
655 biosynthesis, the climacteric respiration peak, and consequent ripening-related trait development,  
656 independent of prior ethylene sensitivity [34, 110]. A mechanism for the observed variation in  
657 AOX transcripts between the tested pear cultivars and other model climacteric systems is  
658 unclear, though such variation in AOX expression and activity has been reported in many plants  
659 for some time [111, 112].

660  
661 *Comparative gene expression analyses using LinReg PCR-corrected 2-( $\Delta\Delta$ Ct)*  
662 The LinRegPCR workflow was applied to the 2-( $\Delta\Delta$ Ct) expression data for 27 genes. A heatmap  
663 of the relative expression was produced using Morpheus (Broad Institute, 2019), which  
664 illustrates variable patterns of selected genes between ‘Bartlett’ and ‘D’Anjou’ (Figure 5).  
665 Nearly half of the genes included for final analysis exhibited down-regulation throughout fruit

666 phenology in ‘Bartlett’ and ‘D’Anjou’ samples relative to harvest samples. The second half of  
 667 genes exhibited upregulation, exhibiting cultivar or conditioning treatment-dependent deviations.  
 668



669 **Figure 5.** Fold-change gene expression values (from -3 to +3) of topmost variably expressed genes from  
 670 the qRT-PCR analysis in D’Anjou (columns 1-5), and Bartlett (columns 6-10), following sorting from  
 671 final NMDS ordination. Grey cells indicate that a gene was not detected in the sample. \*-indicates 'low  
 672 confidence' values, defined as those from which mean Cq equaled or exceeded 35.00, or whose efficiency  
 673 exceeded 1.80-2.20 in at least one replicate reactions. Gene annotations on right side of the heatmap,  
 674 labeled as letters A-G. A- cold signaling, B- transcriptional regulators, C- ethylene signaling, D- auxin  
 675 signaling, E- abscisic acid signaling, F- peroxisomal or mitochondrial metabolite transport and  
 676 respiration-related, G- internal controls. BH and AH – ‘Bartlett’ and ‘D’Anjou’ fruit two days after  
 677 harvest; BC, AC - ‘Bartlett’ and ‘D’Anjou fruit at 100% conditioning timepoint; ‘BNC, ANC - ‘Bartlett’  
 678 and ‘D’Anjou’ Non- Conditioned control fruit corresponding to 100% conditioning timepoint for fruit  
 679 that received conditioning; BR, AR - ‘Bartlett’ and ‘D’Anjou’ fruit at 100% Ripened stage; BNR, ANR -  
 680 ‘Bartlett’ and ‘D’Anjou’ Non-Conditioned control fruit corresponding to 100% ripening timepoint for  
 681 fruit that received conditioning. Heatmap generated with Morpheus with additional sample and pathways  
 682 annotated using Microsoft PowerPoint. Raw Morpheus output is available in Supplementary file 13.  
 683

684  
 685 Variable transcript abundance at the fully conditioned stage was evident for NCED-, ABI3- and  
 686 ARF-like ‘D’Anjou’ transcripts (columns 2 and 3 of Figure 5). Similar results were apparent for  
 687 ‘Bartlett’ (columns 7 and 8), with variability in response to conditioning evident for FUL1,

688 ACS2, RAN1, ARF5, and CYP707A2-like transcripts. ‘Bartlett’ tissues exhibited generally  
689 higher AOX1 and AOX2 transcript abundance, suggesting that AOX induction in ‘D’Anjou’  
690 may be muted. Enhanced AOX transcript abundance and activity has been associated with  
691 accelerated ripening in other climacteric systems in which S2 ethylene-production is impaired  
692 [35, 106]. These results highlight shared and unique transcriptional responses in these two  
693 cultivars that have a very different conditioning requirement for the transition to S2.

694

695 In this analysis approach, increased AOX-like transcript abundance coincided with that of ACS,  
696 ARF, and ABA-related genes for ‘Bartlett’ and ‘D’Anjou’ samples, suggesting that these  
697 pathways comprise at least part of a coordinated transcriptional cascade that results in S2  
698 ethylene biosynthesis and acquisition of ripening competency (Figure 5). In this role, induction  
699 of the AOX pathway in pear may provide an additional hub of regulatory control beyond the  
700 MADS-RIN complex, which integrates signals from cold-signaling pathways, while relieving  
701 limited energy production and metabolic flux from the mitochondria. Some initial work in  
702 climacteric systems suggests this control point could affect increased ethylene biosynthesis  
703 through a retrograde signal derived from respiratory activity, metabolic flux or energy limitation  
704 [112]. The cold and phytohormone-responsive transcriptional activator MYB29 was shown in  
705 Arabidopsis to be a putative regulator of AOX activity via such a retrograde signaling  
706 mechanism, integrating numerous hormonal and signaling pathways with respiration [113].  
707 MYB29-like and other R2R3-MYB genes have only recently been the subject of broad  
708 comparative analyses in other climacteric crops [114] and can be found in *P. communis* and *P.*  
709 *bretschneideri* genomes. Such genes were also found to be a target of miRNAs influencing post-  
710 cold storage physiological responses in Litchi [115].

711

712 Adding to this, sulfur signaling in plants may closely impact respiratory activity, oxidative  
713 signaling, ethylene signaling and may interact with nitric oxide pathways [116-119]. Among the  
714 most variably abundant transcripts in this work was the plastid-derived Rhodanese-like domain-  
715 containing protein 14, a sulfurtransferase localized to the thylakoid. The full complement of the  
716 functional relevance of this protein in plants is unclear, though, after full conditioning treatment,  
717 more of this transcript was found relative to ‘Bartlett’ tissue, which generally loses green  
718 pigmentation more rapidly upon ripening onset than ‘D’Anjou’. Overall, these data, along with  
719 results of other recent studies, presents the possibility that in European pear and other climacteric  
720 fruit, variation in respiratory and phytohormone-pathway activity is not just a consequence of  
721 environmental factors, but also mediates physiological responses to them. Generally, the results  
722 from LinReg PCR-corrected 2-( $\Delta\Delta Ct$ ) correspond to what was observed with the NMDS  
723 approach.

724

725 Utilizing a targeted gene approach, this study allowed for focused analysis of genes documented  
726 to play important roles in cold-induced conditioning and subsequent ripening in pear. It does not,  
727 however, capture transcript abundance of the breadth of genes including those regulating S2-  
728 ethylene and ripening related chromatin modifications, epigenetic regulation or small RNAs, all  
729 of which have been reported to impact these processes in model fruit systems.

730

### 731 *Conclusions*

732 This study adds cultivar specific information regarding the response of European pear to cold  
733 conditioning and lends insight into the genetic changes that occur as fruit transitions to S2



734 ethylene production. Results of this work indicate that cold-sensing and signaling elements from  
735 ABA and auxin pathways modulate S1-S2 ethylene transition in European pears, and suggest  
736 that, while ‘D’Anjou’ pear is able to mitigate and cope with the effects of cold exposure,  
737 ‘Bartlett’ is comparatively less-equipped, resulting in a more pronounced S1-S2 ethylene  
738 biosynthesis transition. Interestingly, enhanced alternative oxidase transcript abundance in  
739 ‘Bartlett’ and ‘D’Anjou’ tissues at the peak of the conditioning treatments suggests that AOX  
740 plays a novel role in the achievement of ripening competency in European pear.

741

## 742 **Acknowledgments**

743 The authors thank Blue Star Growers (Cashmere, WA USA) for providing fruit used for this  
744 study and to D. Scott Mattinson for assistance in the maintenance of the experimental  
745 infrastructure. Work in the Dhingra lab was supported in part by Washington State University  
746 Agriculture Center Research Hatch Grant WNP00011 and grant funding from Pear Bureau NW  
747 to AD. SLH acknowledges the support received from ARCS Seattle Chapter and National  
748 Institutes of Health/National Institute of General Medical Sciences through an institutional  
749 training grant award T32-GM008336. The contents of this work are solely the responsibility of  
750 the authors and do not necessarily represent the official views of the NIGMS or NIH.

751

## 752 **Supplementary Files**

753 Supplementary file 1. ‘Bartlett’ and ‘D’Anjou’ pear flesh firmness raw data and ANOVA  
754 analysis.

755 Supplementary file 2. Quantitative RT-PCR reaction conditions, thermal profile.

756 Supplementary file 3. Quantitative RT-PCR primer names, primer sequences, (Sanger)  
757 sequenced amplicons used and reference providing ab initio annotation to candidate regulatory  
758 transcript(s).

759 Supplementary file 4. LinRegPCR input as raw fluorescence readings from the qRT-PCR  
760 instrument and PCR cycle, with resulting efficiency and Cq output with regression statistics  
761 (Ramakers et al., 2003). LinRegPCR run in plate-wide mean calculation mode. Data separated  
762 by tabs as input and output for each plate run in the qRT-PCR analysis.

763 Supplementary file 5. Initial NMDS ordination of fold-change values from initial qRT-PCR  
764 reaction replicates from all gene targets.

765 Supplementary file 6. NormFinder candidate reference gene input and output.

766 Supplementary file 7. Community master data matrix for initial and final NMDS ordination.

767 Supplementary file 8. Stress plots from initial and final NMDS ordination plot. Stress plots of the  
768 initial (circles) and second (triangles) NMDS ordination procedures. Both instances produced a  
769 final stress coefficient of nearly 0.20 after 20 iterations.

770 Supplementary file 9. Raw R code, NMDS modeling.

771 Supplementary file 10. The radial distance of 90 gene targets from initial NMDS ordination plot  
772 vertex, representing total variability as a function of ripeness and pear cultivar. The radial  
773 distance of final 36 gene targets from final NMDS ordination plot vertex, representing total  
774 variability as a function of pear cultivar and ripeness (NMDS axes 1 and 2, respectively). For  
775 NMDS-2, table of the radial distance of final 36 gene targets from initial NMDS ordination plot  
776 vertex, representing total variability as a function of pear cultivar and ripeness (NMDS axes 1  
777 and 2, respectively).

778 Supplementary file 11. Raw R output, centroid hull plot from 36 genes following initial NMDS  
779 ordination plot representing total Cq variability by treatment group as a function of pear cultivar  
780 and ripeness (NMDS axes 1 and 2, respectively).  
781 Supplementary file 12. Raw R output, final 12 gene set vector plot following final NMDS  
782 ordination plot from the vertex, representing total Cq variability as a function of pear cultivar and  
783 ripeness (NMDS axes 1 and 2, respectively).  
784 Supplementary file 13. Raw Morpheus heatmap tool output in PDF format.  
785

## 786 **References**

- 787 1. White PJ. Recent advances in fruit development and ripening: an overview. *Journal of*  
788 *Experimental Botany*. 2002;53(377):1995-2000. doi: 10.1093/jxb/erf105.
- 789 2. Anwar R, Mattoo AK, Handa AK. Ripening and Senescence of Fleshy Fruits. Paliyath G, J.  
790 Subramanian, L. Lim, K. Subramanian, Handa AK, Mattoo AK, editors2018. 15-51 p.
- 791 3. Karlova R, Chapman N, David K, Angenent GC, Seymour GB, de Maagd RA. Transcriptional  
792 control of fleshy fruit development and ripening. *Journal of Experimental Botany*. 2014;65(16):4527-41.  
793 doi: 10.1093/jxb/eru316.
- 794 4. Granell A, Rambla José L. Biosynthesis of Volatile Compounds. *The Molecular Biology and*  
795 *Biochemistry of Fruit Ripening*. 2013. doi: doi:10.1002/9781118593714.ch6  
796 10.1002/9781118593714.ch6.
- 797 5. Cherian S, Figueroa CR, Nair H. 'Movers and shakers' in the regulation of fruit ripening: a cross-  
798 dissection of climacteric versus non-climacteric fruit. *Journal of Experimental Botany*. 2014;65(17):4705-  
799 22. doi: <https://doi.org/10.1093/jxb/eru280>.
- 800 6. S F Yang a, Hoffman NE. Ethylene Biosynthesis and its Regulation in Higher Plants. *Annual*  
801 *Review of Plant Physiology*. 1984;35(1):155-89. doi: 10.1146/annurev.pp.35.060184.001103.
- 802 7. Tatsuki M. Ethylene Biosynthesis and Perception in Fruit. *Journal of the Japanese Society for*  
803 *Horticultural Science*. 2010;79(4):315-26. PubMed PMID: WOS:000283277200001.
- 804 8. Barry CS, Giovannoni JJ. Ethylene and fruit ripening. *Journal of Plant Growth Regulation*.  
805 2007;26(2):143-59. doi: 10.1007/s00344-007-9002-y. PubMed PMID: WOS:000248582800006.
- 806 9. Barry CS, Llop-Tous MI, Grierson D. The Regulation of 1-Aminocyclopropane-1-Carboxylic Acid  
807 Synthase Gene Expression during the Transition from System-1 to System-2 Ethylene Synthesis in  
808 Tomato. *Plant Physiology*. 2000;123(3):979.
- 809 10. Tucker G, Yin XR, Zhang AD, Wang MM, Zhu QG, Liu XF, et al. Ethylene and fruit softening. *Food*  
810 *Quality & Safety*. 2017;1(4):253-67. doi: 10.1093/fqsafe/fyx024. PubMed PMID:  
811 WOS:000424579100002.
- 812 11. Han Y, Kuang J, Chen J, Liu X, Xiao Y, Fu C, et al. Banana Transcription Factor MaERF11 Recruits  
813 Histone Deacetylase MaHDA1 and Represses the Expression of MaACO1 and Expansins during Fruit  
814 Ripening. *Plant Physiology*. 2016;168(1):357-76. doi: <http://dx.doi.org/10.1104/pp.16.00301>.
- 815 12. Liu M, Pirrello J, Kesari R, Mila I, Roustan JP, Li Z, et al. A dominant repressor version of the  
816 tomato Sl-ERF. B3 gene confers ethylene hypersensitivity via feedback regulation of ethylene signaling  
817 and response components. *The Plant Journal*, 76(3), 406-419. *The Plant Journal*. 2013;73(6):406-19. doi:  
818 10.1111/tbj.12305.
- 819 13. Xiao YY, Chen JY, Kuang JF, Shan W, Xie H, Jiang YM, et al. Banana ethylene response factors are  
820 involved in fruit ripening through their interactions with ethylene biosynthesis genes. *Journal of*  
821 *experimental botany*, 64(8), 2499-2510. *Journal of Experimental Botany*. 2013;64(8). doi:  
822 <https://doi.org/10.1093/jxb/ert108>.

- 823 14. Zhou M, Guo S, Zhang J, Zhang H, Li C, Tang X, et al. Comparative dynamics of ethylene  
824 production and expression of the ACS and ACO genes in normal-ripening and non-ripening watermelon  
825 fruits. *Acta Physiologiae Plantarum*. 2016;38(9). doi: 10.1007/s11738-016-2248-x.
- 826 15. El-Sharkawy I, Sherif S, Mahboob A, Abubaker K, Bouzayen M, Jayasankar S. Expression of auxin-  
827 binding protein1 during plum fruit ontogeny supports the potential role of auxin in initiating and  
828 enhancing climacteric ripening. *Plant Cell Reports*. 2012;31(10):1911-21. doi: 10.1007/s00299-012-1304-  
829 2.
- 830 16. Leng P, Yuan B, Guo YD. The role of abscisic acid in fruit ripening and responses to abiotic stress.  
831 *Journal of Experimental Botany*. 2014;65(16):4577-88. doi: 10.1093/jxb/eru204. PubMed PMID:  
832 WOS:000342928000008.
- 833 17. Soto A, Ruiz, K. B., Ravaglia, D., Costa, G., & Torrigiani, P. . ABA may promote or delay peach fruit  
834 ripening through modulation of ripening-and hormone-related gene expression depending on the  
835 developmental stage. *Plant Physiology and Biochemistry*. 2013;64:11-24. doi: *Plant Physiology and*  
836 *Biochemistry*.
- 837 18. Weng L, Zhao F, Li R, Xu C, Chen K, Xiao H. The Zinc Finger Transcription Factor SIZFP2 Negatively  
838 Regulates Abscisic Acid Biosynthesis and Fruit Ripening in Tomato. *Plant Physiology*. 2015;167(3):931-49.  
839 doi: <http://dx.doi.org/10.1104/pp.114.255174>.
- 840 19. Jia H, Jiu S, Zhang C, Wang C, Tariq P, Liu Z, et al. Abscisic acid and sucrose regulate tomato and  
841 strawberry fruit ripening through the abscisic acid-stress-ripening transcription factor. *Plant*  
842 *biotechnology journal*. 2016;14(10):2045-65. Epub 2016/05/04. doi: 10.1111/pbi.12563. PubMed PMID:  
843 27005823.
- 844 20. Dai S, Li P, Chen P, Li Q, Pei Y, He S, et al. Transcriptional regulation of genes encoding ABA  
845 metabolism enzymes during the fruit development and dehydration stress of pear 'Gold Nijisseiki'. *Plant*  
846 *Physiology and Biochemistry*. 2014;82:299-308. doi: 10.1016/j.plaphy.2014.06.013.
- 847 21. Pons C, Martí C, Forment J, Crisosto CH, Dandekar AM, Granell A. A bulk segregant gene  
848 expression analysis of a peach population reveals components of the underlying mechanism of the fruit  
849 cold response. *PLoS One*. 2014;9(3). doi: <https://doi.org/10.1371/journal.pone.0090706>.
- 850 22. Rahman A. Auxin: a regulator of cold stress response. *Physiol Plantarum*. 2013;147(1):28-35. doi:  
851 10.1111/j.1399-3054.2012.01617.x.
- 852 23. Ashraf MA, Rahman A. Hormonal Regulation of Cold Stress Response. In: Wani SH, Herath V,  
853 editors. *Cold Tolerance in Plants: Physiological, Molecular and Genetic Perspectives*. Cham: Springer  
854 International Publishing; 2018. p. 65-88.
- 855 24. El-Sharkawy I, Sherif S, Mila I, Bouzayen M, Jayasankar S. Molecular characterization of seven  
856 genes encoding ethylene-responsive transcriptional factors during plum fruit development and ripening.  
857 *Journal of Experimental Botany*. 2009;60(3):907-22. doi: <https://doi.org/10.1093/jxb/ern354>.
- 858 25. Tatsuki M, Nakajima N, Fujii H, Shimada T, Nakano M, Hayashi K-I, et al. Increased levels of IAA  
859 are required for system 2 ethylene synthesis causing fruit softening in peach (*Prunus persica* L. Batsch).  
860 *Journal of Experimental Botany*. 2013;64(6):1049-59. doi: <https://doi.org/10.1093/jxb/ers381>.
- 861 26. Yang Y, Wu Y, Pirrello J, Regad F, Bouzayen M, Deng W, et al. Silencing SI-EBF1 and SI-EBF2  
862 expression causes constitutive ethylene response phenotype, accelerated plant senescence, and fruit  
863 ripening in tomato. *Journal of Experimental Botany*. 2009;61(3):697-708. doi:  
864 <https://doi.org/10.1093/jxb/erp332>.
- 865 27. Choudhury SR, Roy S, Sengupta DN. Characterization of transcriptional profiles of MA-ACS1 and  
866 MA-ACO1 genes in response to ethylene, auxin, wounding, cold and different photoperiods during  
867 ripening in banana fruit. *J Plant Physiol*. 2008;165(18):1865-78. doi:  
868 <http://doi.org/10.1016/j.jplph.2008.04.012>.

- 869 28. Fujisawa M, Nakano T, Shima Y, Ito Y. A large-scale identification of direct targets of the tomato  
870 MADS box transcription factor RIPENING INHIBITOR reveals the regulation of fruit ripening. *The Plant*  
871 *Cell*. 2013;25(3):371-86. doi: <http://dx.doi.org/10.1105/tpc.112.108118>.
- 872 29. Ito Y, Nishizawa-Yokoi A, Endo M, Mikami M, Shima Y, Nakamura N, et al. Re-evaluation of the  
873 rin mutation and the role of RIN in the induction of tomato ripening. *Nature Plants*. 2017;3(11):866-74.  
874 doi: [10.1038/s41477-017-0041-5](https://doi.org/10.1038/s41477-017-0041-5).
- 875 30. Elitzur T, Yakir E, Quansah L, Zhangjun F, Vrebalob JT, Khayat E, et al. Banana MaMADS  
876 transcription factors are necessary for fruit ripening and molecular tools to promote shelf-life and food  
877 security. *Plant Physiology*. 2016. doi: <http://dx.doi.org/10.1104/pp.15.01866>.
- 878 31. Osorio S, Scossa F, Fernie AR. Molecular regulation of fruit ripening. *Front Plant Sci*. 2013;4. doi:  
879 <https://doi.org/10.3389/fpls.2013.00198>.
- 880 32. Nham NT, Macnish AJ, Zakharov F, Mitcham EJ. 'Bartlett' pear fruit (*Pyrus communis* L.) ripening  
881 regulation by low temperatures involves genes associated with jasmonic acid, cold response, and  
882 transcription factors. *Plant Science*. 2017;260:8-18. doi: <https://doi.org/10.1016/j.plantsci.2017.03.008>.
- 883 33. Berkowitz O, De Clercq I, Van Breusegem F, Whelan J. Interaction between hormonal and  
884 mitochondrial signalling during growth, development and in plant defence responses. *Plant, Cell and*  
885 *Environment*. 2016;39(5):1127-39. doi: [10.1111/pce.12712](https://doi.org/10.1111/pce.12712).
- 886 34. Perotti VE, Moreno AS, Podestá FE. Physiological aspects of fruit ripening: the mitochondrial  
887 connection. *Mitochondrion*. 2014;17:1-6. doi: [Mitochondrion](https://doi.org/10.1016/j.mito.2014.05.001).
- 888 35. Dhingra A, Hendrickson C, inventorsControl of ripening and senescence in pre-harvest and post-  
889 harvest plants and plant materials by manipulating alternative oxidase activity. USA patent 9,591,847.  
890 2017.
- 891 36. Considine MJ, Daley DO, Whelan J. The expression of alternative oxidase and uncoupling protein  
892 during fruit ripening in mango. *Plant Physiol*. 2001;126(4):1619-29. doi: [http://dx.doi.org/10.1104/pp.](http://dx.doi.org/10.1104/pp.126.4.1619)  
893 [126.4.1619](http://dx.doi.org/10.1104/pp.126.4.1619).
- 894 37. Duque P, Arrabaca JD. Respiratory metabolism during cold storage of apple fruit. II. Alternative  
895 oxidase is induced at the climacteric. *Physiol Plantarum*. 1999;107(1):24-31. doi: DOI 10.1034/j.1399-  
896 3054.1999.100104.x. PubMed PMID: ISI:000083523200004.
- 897 38. Holtzapffel RC, M Finnegan P, Millar A, R Badger M, Day D. Mitochondrial protein expression in  
898 tomato fruit during on-vine ripening and cold storage2002. 827-34 p.
- 899 39. Lei T, Feng H, Sun X, Dai Q-L, Zhang F, Liang H-G, et al. The alternative pathway in cucumber  
900 seedlings under low temperature stress was enhanced by salicylic acid. *Plant Growth Regul*.  
901 2009;60(1):35. doi: [10.1007/s10725-009-9416-6](https://doi.org/10.1007/s10725-009-9416-6).
- 902 40. Yang Q-S, Wu J-H, Li C-Y, Wei Y-R, Sheng O, Hu C-H, et al. Quantitative proteomic analysis reveals  
903 that antioxidation mechanisms contribute to cold tolerance in plantain (*Musa paradisiaca* L.; ABB Group)  
904 seedlings. *Molecular & cellular proteomics : MCP*. 2012;11(12):1853-69. Epub 2012/09/16. doi:  
905 [10.1074/mcp.M112.022079](https://doi.org/10.1074/mcp.M112.022079). PubMed PMID: 22982374.
- 906 41. Jobling JJ, McGlasson WB. A comparison of ethylene production, maturity and controlled  
907 atmosphere storage life of Gala, Fuji and Lady Williams apples (*Malus domestica*, Borkh.). *Postharvest*  
908 *Biol Tec*. 1995;6(3):209-18. doi: [https://doi.org/10.1016/0925-5214\(94\)00002-A](https://doi.org/10.1016/0925-5214(94)00002-A).
- 909 42. Knee M, Looney NE, Hatfield SGS, Smith SM. Initiation of Rapid Ethylene Synthesis by Apple and  
910 Pear Fruits in Relation to Storage Temperature. *Journal of Experimental Botany*. 1983;34(146):1207-12.
- 911 43. Hershkovitz V, Friedman H, Goldschmidt EE, Feygenberg O, Pesis E. Induction of ethylene in  
912 avocado fruit in response to chilling stress on tree. *J Plant Physiol*. 2009;166(17):1855-62. Epub  
913 2009/07/14. doi: [10.1016/j.jplph.2009.05.012](https://doi.org/10.1016/j.jplph.2009.05.012). PubMed PMID: 19592132.
- 914 44. Mworio EG, Yoshikawa T, Salikon N, Oda C, Asiche WO, Yokotani N, et al. Low-temperature-  
915 modulated fruit ripening is independent of ethylene in 'Sanuki Gold' kiwifruit. *Journal of Experimental*  
916 *Botany*. 2012;63(2):963-71. doi: [10.1093/jxb/err324](https://doi.org/10.1093/jxb/err324). PubMed PMID: PMC3254691.

- 917 45. Lelievre JM, Tichit L, Dao P, Fillion L, Nam YW, Pech JC, et al. Effects of chilling on the expression  
918 of ethylene biosynthetic genes in Passe-Crassane pear (*Pyrus communis* L.) fruits. *Plant Mol Biol*.  
919 1997;33(5):847-55. Epub 1997/03/01. PubMed PMID: 9106508.
- 920 46. Hartmann C, Drouet A, Morin F. Ethylene and ripening of apple, pear and cherry fruit. *Plant*  
921 *Physiology and Biochemistry*. 1987;25(4):505-12.
- 922 47. Sugar D, Einhorn TC. Conditioning temperature and harvest maturity influence induction of  
923 ripening capacity in 'd'Anjou' pear fruit. *Postharvest Biol Tec*. 2011;60(2):121-4. doi:  
924 <http://doi.org/10.1016/j.postharvbio.2010.12.005>.
- 925 48. Sugar D, Basile SR. Integrated ethylene and temperature conditioning for induction of ripening  
926 capacity in 'Anjou' and 'Comice' pears. *Postharvest Biol Tec*. 2013;83:9-16. doi:  
927 <http://doi.org/10.1016/j.postharvbio.2013.03.010>.
- 928 49. Sugar D, Basile SR, editors. Integrated ethylene and temperature conditioning for inducing pear  
929 ripening capacity 2015: International Society for Horticultural Science (ISHS), Leuven, Belgium.
- 930 50. Chiriboga MA, Schotsmans WC, Larrigaudière C, Dupille E, Recasens I. Responsiveness of  
931 'Conference' pears to 1-methylcyclopropene: the role of harvest date, orchard location and year. *Journal*  
932 *of Science of Food and Agriculture*. 2013;93(3):619-25. doi: 10.1002/jsfa.5853.
- 933 51. Zucoloto M, Antonioli LR, Squeira DL, Czermainski ABC, Salomao LCC. Conditioning temperature  
934 for inducing uniform ripening of 'Abate Fetel' pears. *Revista Ciência Agronômica*. 2016;47(2):344-50.  
935 doi: 10.5935/1806-6690.20160040.
- 936 52. Smékalová V, Doskočilová A, Komis G, Šamaj J. (2014). Crosstalk between secondary  
937 messengers, hormones and MAPK modules during abiotic stress signalling in plants. , 32(1), 2-11.  
938 *Biotechnology Advances*. 2014;32(1):2-11. doi: <http://doi.org/10.1016/j.biotechadv.2013.07.009>.
- 939 53. Nham NT, Willits N, Zakharov F, Mitcham EJ. A model to predict ripening capacity of 'Bartlett'  
940 pears (*Pyrus communis* L.) based on relative expression of genes associated with the ethylene pathway.  
941 *Postharvest Biol Tec*. 2017;128:138-43. doi: <https://doi.org/10.1016/j.postharvbio.2017.02.006>.
- 942 54. Nham NT, de Fretas ST, Macnish AJ, Carr KM, Kietikul T, Guilatco AJ, et al. A transcriptome  
943 approach towards understanding the development of ripening capacity in 'Bartlett' pears (*Pyrus*  
944 *communis* L.). *Bmc Genomics*. 2015;16(1). doi: 10.1186/s12864-015-1939-9.
- 945 55. Paul V, Pandey R, Srivastava GC. The fading distinctions between classical patterns of ripening in  
946 climacteric and non-climacteric fruit and the ubiquity of ethylene—an overview. *Journal of Food Science*  
947 *and Technology*. 2012;49(1):1-21. doi: 10.1007/s13197-011-0293-4.
- 948 56. Catala R, Medina J, Salinas J. Integration of low temperature and light signaling during cold  
949 acclimation response in *Arabidopsis*. *Proc Natl Acad Sci U S A*. 2011;108(39):16475-80. Epub  
950 2011/09/21. doi: 10.1073/pnas.1107161108. PubMed PMID: 21930922; PubMed Central PMCID:  
951 PMC3182711.
- 952 57. Kondo S, Meemak S, Ban Y, Moriguchi T, Harada T. Effects of auxin and jasmonates on 1-  
953 aminocyclopropane-1-carboxylate (ACC) synthase and ACC oxidase gene expression during ripening of  
954 apple fruit. *Postharvest Biol Tec*. 2009;51(2):281-4. doi:  
955 <http://doi.org/10.1016/j.postharvbio.2008.07.012>.
- 956 58. Tacken EJ, Ireland HS, Wang YY, Putterill J, Schaffer RJ. Apple EIN3 BINDING F-box 1 inhibits the  
957 activity of three apple EIN3-like transcription factors. . *AoB Plants*. 2012. doi:  
958 <https://doi.org/10.1093/aobpla/pls034>.
- 959 59. McCune B, Grace J. Analysis of ecological communities. MJM Software Design, Gleneden Beach,  
960 OR2002.
- 961 60. Donoho D. High-Dimensional Data Analysis: The Curses and Blessings of Dimensionality 2000. 1-  
962 32 p.



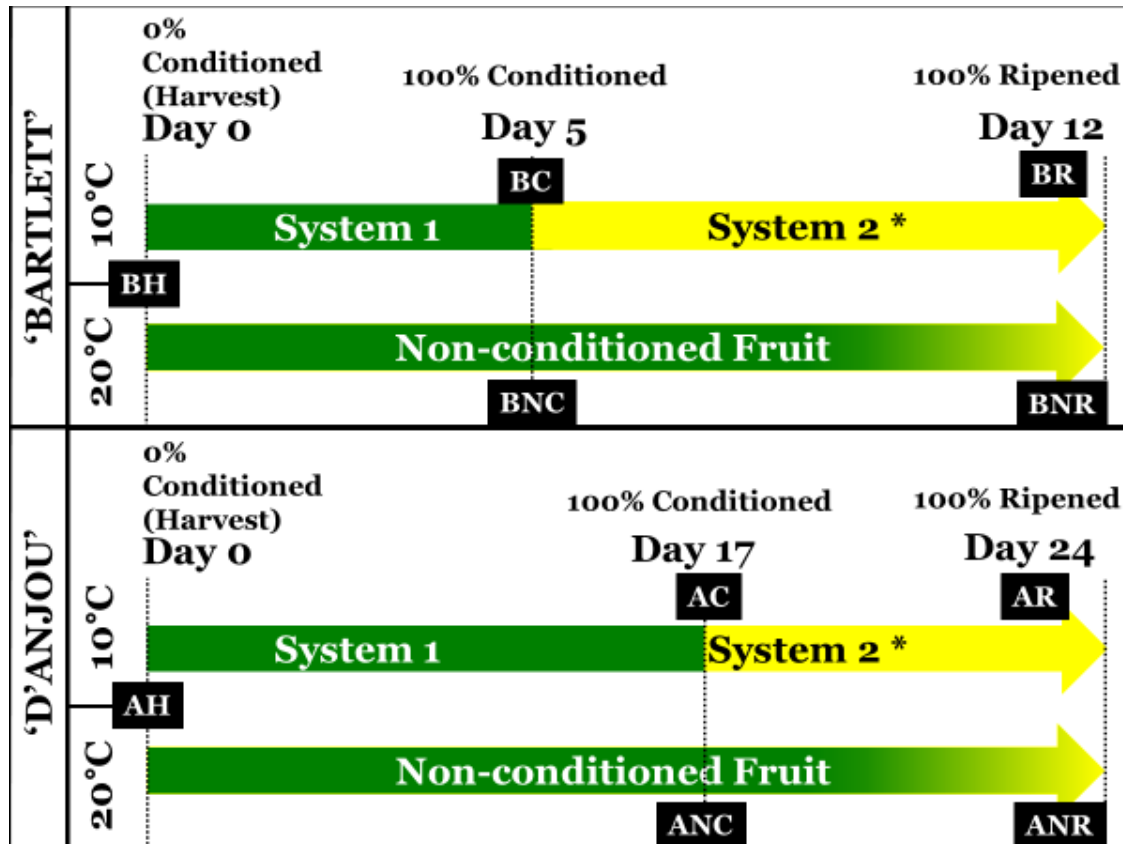
- 963 61. Val J, Monge E, Risco D, Blanco A. Effect of Pre-Harvest Calcium Sprays on Calcium  
964 Concentrations in the Skin and Flesh of Apples. *Journal of Plant Nutrition*. 2008;31(11):1889-905. doi:  
965 10.1080/01904160802402757.
- 966 62. Dhingra A. Pre-publication Release of Rosaceae Genome Information  
967 <https://genomics.wsu.edu/research/> Washington State University; 2013 [cited 2016 December 10].  
968 Available from: <https://genomics.wsu.edu/research/>
- 969 63. Velasco R, Zharkikh A, Affourtit J, Dhingra A, Cestaro A, Kalyanaraman A, et al. The genome of  
970 the domesticated apple (*Malus [times] domestica* Borkh.). *Nature genetics*. 2010;42(10):833-9.
- 971 64. Kruskal JB. Nonmetric multidimensional scaling: A numerical method. *Psychometrika*.  
972 1964;29(2):115-29. doi: 10.1007/bf02289694.
- 973 65. Oksanen JRpv, 1(7), 11-12. Multivariate analysis of ecological communities in R: vegan tutorial. R  
974 Package version. 2011;1(7):11-2.
- 975 66. Krzywinski M, Altman N. Points of significance: Nonparametric tests. *Nature Methods*.  
976 2014;11(5):467-8. doi: 10.1038/nmeth.2937.
- 977 67. Pfaffl MW, Horgan GW, Dempfle L. Relative expression software tool (REST©) for group-wise  
978 comparison and statistical analysis of relative expression results in real-time PCR. *Nucleic Acid Research*.  
979 2002;30(9). doi: <https://doi.org/10.1093/nar/30.9.e36>.
- 980 68. Morpheus. Broad Institute <https://software.broadinstitute.org/morpheus2019>.
- 981 69. USDA. Agricultural Statistics 2016. USDA NASS; 2016.
- 982 70. Elkins R, Bell R, Einhorn TC. Needs Assessment for Future US Pear Rootstock Research Directions  
983 Based on the Current State of Pear Production and Rootstock Research. *J Am Pom Soc*. 2012;66(3):153-  
984 63.
- 985 71. Guzman D, Dhingra A. Challenges and Opportunities in Pear Breeding. In: Lang G, editor. *Achieving*  
986 *sustainable cultivation of temperate zone tree fruits and berries*. 2. Cambridge, UK: Burleigh Dodd  
987 Science Publishing Limited; 2019.
- 988 72. Minas IS, Tanou G, Molassiotis A. Environmental and orchard bases of peach fruit quality.  
989 *Scientia Horticulturae*. 2018;235:307-22. doi: <https://doi.org/10.1016/j.scienta.2018.01.028>.
- 990 73. Serra S, Sullivan N, Mattheis JP, Musacchi S, Rudell DR. Canopy attachment position influences  
991 metabolism and peel constituency of European pear fruit. *BMC Plant Biology*. 2018;18(1):364. doi:  
992 10.1186/s12870-018-1544-6.
- 993 74. Agar IT, Biasi WV, Mitcham EJ. Temperature and exposure time during ethylene conditioning  
994 affect ripening of Bartlett pears. *J Agric Food Chem*. 2000;48(2):165-70. Epub 2000/02/26. PubMed  
995 PMID: 10691611.
- 996 75. Sugar D, Mitcham E, Kupferman G. Rethinking the chill requirement for pear ripening. *Good*  
997 *Fruit Grower*. 2009.
- 998 76. Villalobos-Acuna M, Mitcham EJ. Ripening of European pears: the chilling dilemma. *Postharvest*  
999 *Biol Tec*. 2008;49(2):187-200. doi: 10.1016/j.postharvbio.2008.03.003. PubMed PMID:  
1000 WOS:000257364600001.
- 1001 77. Rieu I, Powers SJ. Real-time quantitative RT-PCR: design, calculations, and statistics. *Plant Cell*.  
1002 2009;21(4):1031-3. Epub 2009/04/28. doi: 10.1105/tpc.109.066001. PubMed PMID: 19395682; PubMed  
1003 Central PMCID: PMCPMC2685626.
- 1004 78. McCarthy DJ, Smyth GK. Testing significance relative to a fold-change threshold is a TREAT.  
1005 *Bioinformatics*. 2009;25(6):765-71. doi: 10.1093/bioinformatics/btp053.
- 1006 79. Dalman MR, Deeter A, Nimishakavi G, Duan Z-H. Fold change and p-value cutoffs significantly  
1007 alter microarray interpretations. *BMC Bioinformatics*. 2012;13(2):S11. doi: 10.1186/1471-2105-13-s2-  
1008 s11.
- 1009 80. Ho J, Tumkaya T, Aryal S, Choi H, Claridge-Chang A. Moving beyond  $P$  values:  
1010 Everyday data analysis with estimation plots. *bioRxiv*. 2019:377978. doi: 10.1101/377978.

- 1011 81. Jajo A, Rahim MA, Serra S, Gagliardi F, Jajo NK, Musacchi S, et al. Impact of tree training system,  
1012 branch type and position in the canopy on the ripening homogeneity of 'Abbé Fétel' pear fruit. *Tree*  
1013 *Genetics & Genomes*. 2014;10(5):1477-88. doi: 10.1007/s11295-014-0777-2.
- 1014 82. Rudell DR, Serra S, Sullivan N, Mattheis JP, Musacchi S. Survey of 'd'Anjou' Pear Metabolic  
1015 Profile Following Harvest from Different Canopy Positions and Fruit Tissues. 2017;52(11):1501. doi:  
1016 10.21273/hortsci12375-17.
- 1017 83. Olsvik PA, Sjøfteland L, Lie KK. Selection of reference genes for qRT-PCR examination of wild  
1018 populations of Atlantic cod *Gadus morhua*. *BMC Research Notes*. 2008;1(1):47. doi: 10.1186/1756-0500-  
1019 1-47.
- 1020 84. Liu M, Udhe-Stone C, Goudar CT. Progress curve analysis of qRT-PCR reactions using the logistic  
1021 growth equation. *Biotechnology progress*. 2011;27(5):1407-14. Epub 2011/07/19. doi:  
1022 10.1002/btpr.666. PubMed PMID: 21766473.
- 1023 85. Nham NT, Macnish AJ, Zakharov F, Mitcham EJ. 'Bartlett' pear fruit (*Pyrus communis* L.) ripening  
1024 regulation by low temperatures involves genes associated with jasmonic acid, cold response, and  
1025 transcription factors. *Plant Science*. 2017;260:8–18. doi: <http://doi.org/10.1016/j.plantsci.2017.03.008>.
- 1026 86. Sharkawy IE-S, Jones B, Gentzbittel L, Lelièvre J-M. Differential regulation of ACC synthase genes  
1027 in cold-dependent and -independent ripening in pear fruit. *Plant, Cell & Environ*. 2004;27(10):1197–210.  
1028 doi: 10.1111/j.1365-3040.2004.01218.x.
- 1029 87. El-Sharkawy E-I, Jones B, Gentzbittel L, Lelivre JM, Pech JC, Latché A. Differential regulation of  
1030 ACC synthase genes in cold-dependent and-independent ripening in pear fruit. *Plant, Cell & Environ*.  
1031 2004;27(10):1197-210. doi: 10.1111/j.1365-3040.2004.01218.x.
- 1032 88. Liu M, Pirrello J, Chervin C, Roustan J-P, Bouzayen M. Ethylene Control of Fruit Ripening:  
1033 Revisiting the Complex Network of Transcriptional Regulation. *Plant Physiology*. 2015;169(4):2380-90.  
1034 doi: 10.1104/pp.15.01361.
- 1035 89. Shan W, Kuang JF, Lu WJ, Chen JY. Banana fruit NAC transcription factor MaNAC1 is a direct  
1036 target of MalCE1 and involved in cold stress through interacting with MaCBF1. *Plant, Cell and*  
1037 *Environment*. 2014;37(9):2116-27. doi: 10.1111/pce.12303.
- 1038 90. Sivankalyani V, Geetha M, Subramanyam K, Girija S. Ectopic expression of Arabidopsis RCI2A  
1039 gene contributes to cold tolerance in tomato. *Transgenic Research*. 2015;24(2):237-51. doi:  
1040 10.1007/s11248-014-9840-x.
- 1041 91. Shi Y, Yang S. ABA Regulation of the Cold Stress Response in Plants. In: Zhang D-P, editor.  
1042 *Abscisic Acid: Metabolism, Transport and Signaling*. Dordrecht: Springer Netherlands; 2014. p. 337-63.
- 1043 92. Eremina M, Rozhon W, Poppenberger B. Hormonal control of cold stress responses in plants.  
1044 *Cellular and Molecular Life Sciences*. 2016;73(4):797-810. doi: 10.1007/s00018-015-2089-6.
- 1045 93. Tian MS, Prakash S, Zhang N, Ross GS. Chilling-induced ethylene biosynthesis in Braeburn apples.  
1046 *Plant Growth Regul*. 2002;38(3):249-57. doi: 10.1023/a:1021552002676.
- 1047 94. Binder BM, Rodríguez FI, Bleecker AB. The copper transporter RAN1 is essential for biogenesis of  
1048 ethylene receptors in Arabidopsis. *Journal of Biological Chemistry*. 2010;285(48):37263-70. doi:  
1049 10.1074/jbc.M110.170027.
- 1050 95. Resnick JS, Wen C-K, Shockey JA, Chang C. REVERSION-TO-ETHYLENE SENSITIVITY1, a  
1051 conserved gene that regulates ethylene receptor function in Arabidopsis. *Proceedings of the*  
1052 *National Academy of Sciences*. 2006;103(20):7917-22. doi: 10.1073/pnas.0602239103.
- 1053 96. Zhang M-Y, Xue C, Xu L, Sun H, Qin M-F, Zhang S, et al. Distinct transcriptome profiles reveal  
1054 gene expression patterns during fruit development and maturation in five main cultivated species of  
1055 pear (*Pyrus* L.). *Scientific Reports*. 2016;6:28130. doi: 10.1038/srep28130
- 1056 <https://www.nature.com/articles/srep28130#supplementary-information>.

- 1057 97. Catalá R, López-Cobollo R, Castellano MM, Angosto T, Alonso JM, Ecker JR, et al. The Arabidopsis  
1058 14-3-3 protein RARE COLD INDUCIBLE 1A links low-temperature response and ethylene biosynthesis to  
1059 regulate freezing tolerance and cold acclimation. *The Plant Cell*. 2014;26(8):3326-42. doi: <http://dx.doi.org/10.1105/tpc.114.127605>.
- 1060  
1061 98. Obsilova V, Kopecka M, Kosek D, Kacirova M, Kylarova S, Rezabkova L, et al. Mechanisms of the  
1062 14-3-3 protein function: regulation of protein function through conformational modulation. *Physiol Res*.  
1063 2014;63 Suppl 1:S155-64. Epub 2014/02/26. PubMed PMID: 24564655.
- 1064 99. Medina J, Rodríguez-Franco M, Peñalosa A, Carrascosa MJ, Neuhaus G, Salinas J. Arabidopsis  
1065 mutants deregulated in RC12A expression reveal new signaling pathways in abiotic stress responses. *The*  
1066 *Plant Journal*. 2005;42(4):586-97. doi: [doi:10.1111/j.1365-3113X.2005.02400.x](https://doi.org/10.1111/j.1365-3113X.2005.02400.x).
- 1067 100. Pattison RJ, Csukasi, F., & Catalá, C. (2014). . Mechanisms regulating auxin action during fruit  
1068 development. *Physiol Plantarum*. 2014;151(1):62-72. doi: [10.1111/ppl.12142](https://doi.org/10.1111/ppl.12142).
- 1069 101. El-Sharkawy I, Sherif SM, Jones B, Mila I, Kumar PP, Bouzayen M, et al. TIR1-like auxin-receptors  
1070 are involved in the regulation of plum fruit development. *Journal of Experimental Botany*.  
1071 2014;65(18):5205-15. doi: <https://doi.org/10.1093/jxb/eru279>.
- 1072 102. Breitel DA, Chappell-Maor L, Meir S, Panizel I, Puig CP, Hao Y, et al. AUXIN RESPONSE FACTOR 2  
1073 Intersects Hormonal Signals in the Regulation of Tomato Fruit Ripening. *PLoS genetics*. 2016;12(3). doi:  
1074 <https://doi.org/10.1371/journal.pgen.1005903>.
- 1075 103. Dong T, Hu Z, Deng L, Wang Y, Zhu M, Zhang J, et al. A tomato MADS-box transcription factor,  
1076 SIMADS1, acts as a negative regulator of fruit ripening. *Plant Physiology*. 2013;163(2):1026-36. doi:  
1077 <http://dx.doi.org/10.1104/pp.113.224436>.
- 1078 104. Bemer M, Karlova R, Ballester AR, Tikunov YM, Bovy AG, Wolters-Arts M, et al. The Tomato  
1079 FRUITFULL Homologs TDR4/FUL1 and MBP7/FUL2 Regulate Ethylene-Independent Aspects of Fruit  
1080 Ripening. *The Plant Cell*. 2012;24(11):4437-51. doi: <http://dx.doi.org/10.1105/tpc.112.103283>.
- 1081 105. Shima Y, Fujisawa M, Kitagawa M, Nakano T, Kimbara J, Nakamura N, et al. Tomato FRUITFULL  
1082 homologs regulate fruit ripening via ethylene biosynthesis. *Bioscience, Biotechnology and Biochemistry*.  
1083 2014;78(2):231-7. doi: <http://dx.doi.org/10.1080/09168451.2014.878221>.
- 1084 106. Xu F, Yuan S, Zhang DW, Lv X, Lin HH. The role of alternative oxidase in tomato fruit ripening and  
1085 its regulatory interaction with ethylene. *J Exp Bot*. 2012;63(15):5705-16. Epub 2012/08/24. doi: [ers226](https://doi.org/10.1093/jxb/ers226)  
1086 [pii]
- 1087 10.1093/jxb/ers226. PubMed PMID: 22915749.
- 1088 107. Borecký J, Nogueira, F. T., De Oliveira, K. A., Maia, I. G., Vercesi, A. E., & Arruda, P. (2006). . The  
1089 plant energy-dissipating mitochondrial systems: depicting the genomic structure and the expression  
1090 profiles of the gene families of uncoupling protein and alternative oxidase in monocots and dicots. .  
1091 *Journal of Experimental Botany*. 2006;57(4):849-64. doi: <https://doi.org/10.1093/jxb/erj070>.
- 1092 108. Feng H, Guan D, Sun K, Wang Y, Zhang T, Wang R. Expression and signal regulation of the  
1093 alternative oxidase genes under abiotic stresses. . *Acta Biochimica et Biophysica Sinica*. 2013;45(12):985-  
1094 94. doi: [10.1093/abbs/gmt094](https://doi.org/10.1093/abbs/gmt094)
- 1095 109. Xu F, Yuan S, Zhang D-W, Lv X, Lin H-H. The role of alternative oxidase in tomato fruit ripening  
1096 and its regulatory interaction with ethylene. *J Exp Bot*. 2012;63(15):5707-16. doi:  
1097 <https://doi.org/10.1093/jxb/ers226>.
- 1098 110. Xu F, Yuan S, Zhang DW, Lv X, Lin HH. The role of alternative oxidase in tomato fruit ripening and  
1099 its regulatory interaction with ethylene. *Journal of Experimental Botany*. 2012;63(15):5705-16. doi:  
1100 <https://doi.org/10.1093/jxb/ers226>.
- 1101 111. Wagner AM. A role for active oxygen species as second messengers in the induction of  
1102 alternative oxidase gene expression in *Petunia hybrida* cells. *FEBS Lett*. 1995;368(2):339-42. Epub  
1103 1995/07/17. PubMed PMID: 7628633.

- 1104 112. Vanlerberghe GC. Alternative Oxidase: A Mitochondrial Respiratory Pathway to Maintain  
1105 Metabolic and Signaling Homeostasis during Abiotic and Biotic Stress in Plants. *International Journal of*  
1106 *Molecular Sciences*. 2013;14(4):6805-47. doi: 10.3390/ijms14046805. PubMed PMID: PMC3645666.
- 1107 113. Zhang X, Ivanova A, Vandepoele K, Radomiljac JD, Van de Velde J, Berkowitz O, et al. The  
1108 transcription factor MYB29 is a regulator of ALTERNATIVE OXIDASE 1. *Plant Physiology*. 2017. doi: [http://](http://dx.doi.org/10.1104/pp.16.01494)  
1109 [dx.doi.org/10.1104/pp.16.01494](http://dx.doi.org/10.1104/pp.16.01494).
- 1110 114. Fan ZQ, Ba LJ, Shan W, Xiao YY, Lu WJ, Kuang JF, et al. A banana R2R3-MYB transcription factor  
1111 MaMYB3 is involved in fruit ripening through modulation of starch degradation by repressing starch  
1112 degradation-related genes and MabHLH6. *Plant J*. 2018;96(6):1191-205. Epub 2018/09/23. doi:  
1113 10.1111/tpj.14099. PubMed PMID: 30242914.
- 1114 115. Yao F, Zhu H, Yi C, Qu H, Jiang Y. MicroRNAs and targets in senescent litchi fruit during ambient  
1115 storage and post-cold storage shelf life. *BMC plant biology*. 2015;15:181-. doi: 10.1186/s12870-015-  
1116 0509-2. PubMed PMID: 26179282.
- 1117 116. Antoniou C, Savvides A, Christou A, Fotopoulos V. Unravelling chemical priming machinery in  
1118 plants: the role of reactive oxygen–nitrogen–sulfur species in abiotic stress tolerance enhancement.  
1119 *Current Opinion in Plant Biology*. 2016;33:101–7. doi: <http://doi.org/10.1016/j.pbi.2016.06.020>.
- 1120 117. Wawrzynska A, Moniuszko G, Sirko A. Links Between Ethylene and Sulfur Nutrition—A  
1121 Regulatory Interplay or Just Metabolite Association? *Front Plant Sci*. 2015;6. doi:  
1122 10.3389/fpls.2015.01053.
- 1123 118. Ziogas V, Molassiotis A, Fotopoulos V, Tanou G. Hydrogen Sulfide: A Potent Tool in Postharvest  
1124 Fruit Biology and Possible Mechanism of Action. *Front Plant Sci*. 2018;9(1375). doi:  
1125 10.3389/fpls.2018.01375.
- 1126 119. Moniuszko G. Ethylene signaling pathway is not linear, however its lateral part is responsible for  
1127 sensing and signaling of sulfur status in plants. *Plant Signal Behav*. 2015;10(11):e1067742. Epub  
1128 2015/09/05. doi: 10.1080/15592324.2015.1067742. PubMed PMID: 26340594; PubMed Central PMCID:  
1129 PMCPMC4883965.
- 1130  
1131

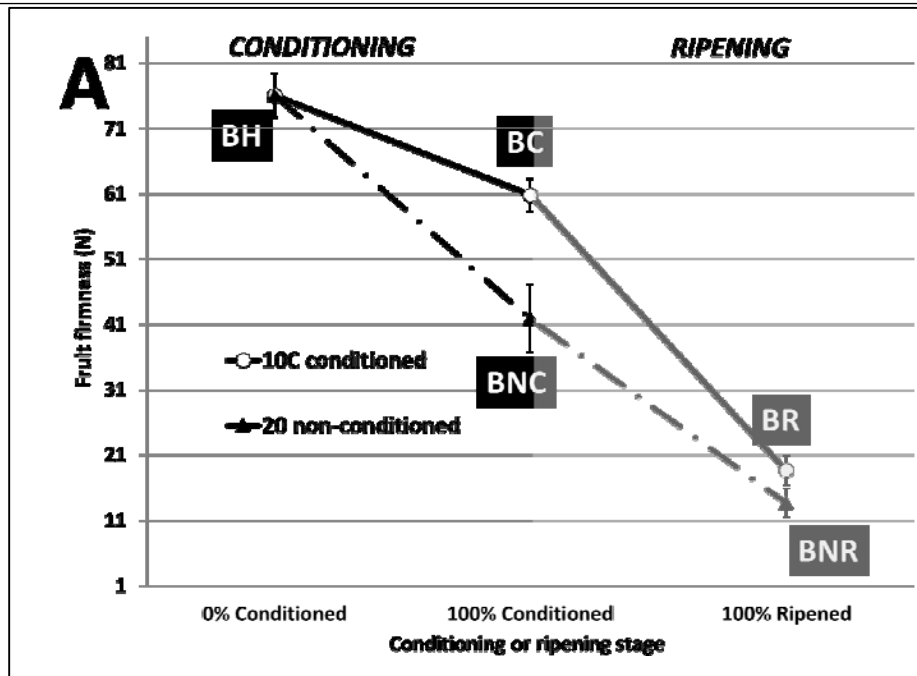
1132 **FIGURES**  
1133



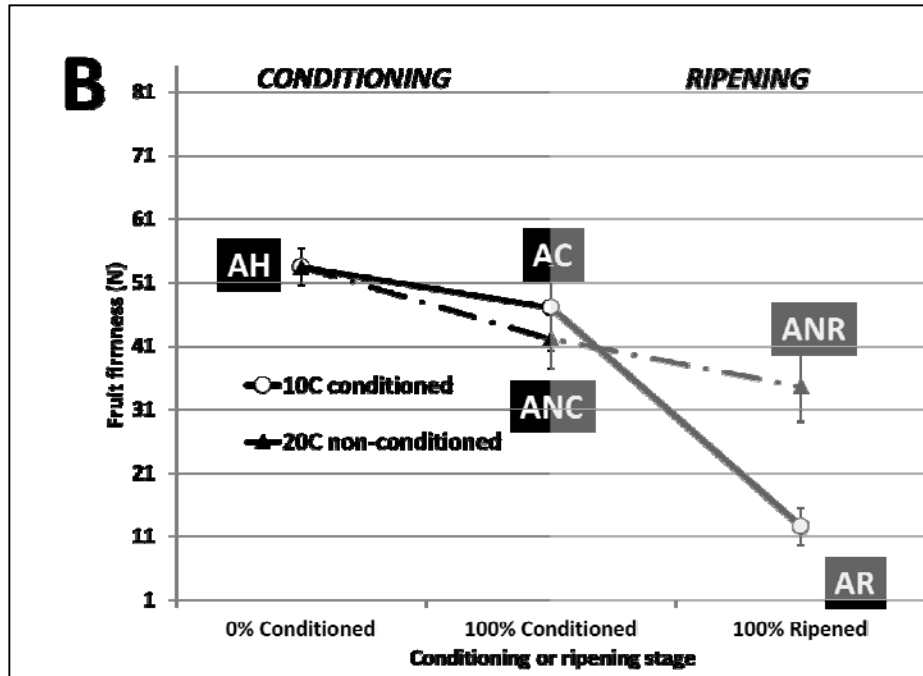
1134



**Figure 1.** Treatment and sampling scheme for ‘Bartlett’ and ‘D’Anjou’ fruit. 1,920 fruit of each cultivar were equally distributed. Tissue samples were obtained from Non-Conditioned control fruit maintained at 20°C in parallel to a sampling of fruit that received conditioning treatment. Conditioned fruit was moved to isolated flow-through respiration chambers at 20°C for one week and samples harvested at that time. BH and AH – ‘Bartlett’ and ‘D’Anjou’ fruit two days after harvest; BC, AC - ‘Bartlett’ and ‘D’Anjou’ fruit at 100% conditioning timepoint; BNC, ANC - ‘Bartlett’ and ‘D’Anjou’ Non-Conditioned control fruit corresponding to 100% conditioning timepoint for fruit that received conditioning; BR, AR - ‘Bartlett’ and ‘D’Anjou’ fruit at 100% Ripened stage; BNR, ANR - ‘Bartlett’ and ‘D’Anjou’ Non-Conditioned control fruit corresponding to 100% ripening timepoint for fruit that received conditioning.



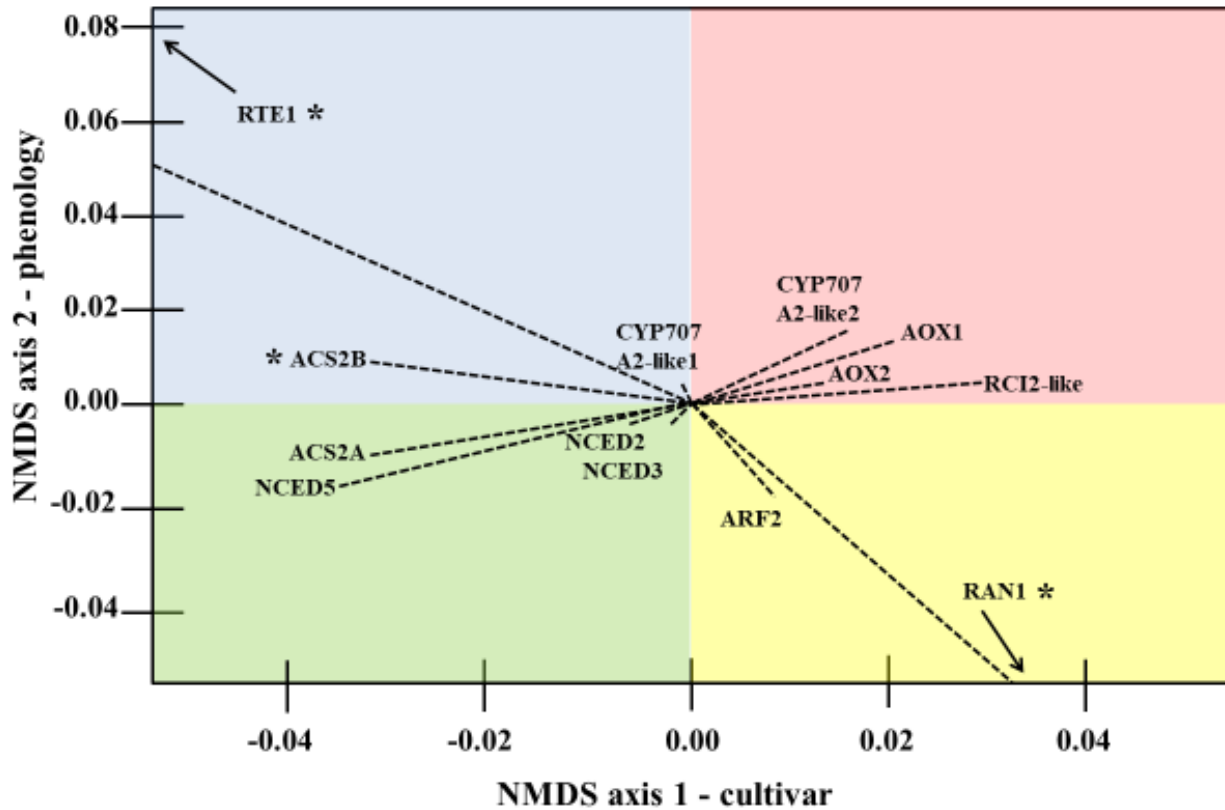
1135



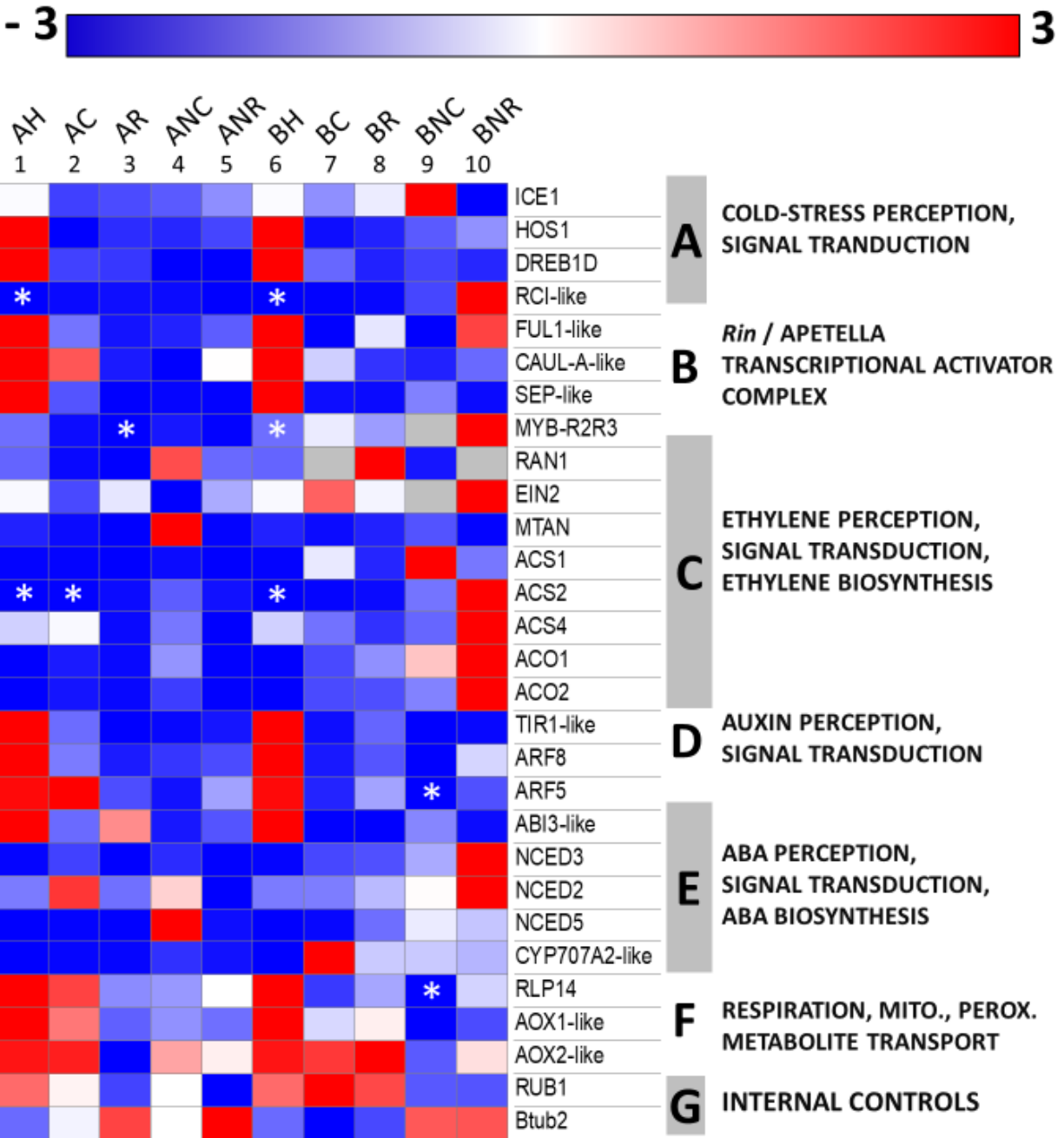
1136  
1137  
1138  
1139  
1140  
1141  
1142  
1143  
1144  
1145  
1146

**Figure 2.** Mean fruit firmness (N) through conditioning (white background) and ripening (grey background) in A. ‘Bartlett’, and B. ‘D’ Anjou’ pear. Fruit was placed into conditioning two days after harvest. Error bars represent standard deviation from the mean of measurements recorded from 10 replicate fruit. Black boxes correspond to fruit treatment sampling stage as follows: BH and AH – ‘Bartlett’ and ‘D’ Anjou’ fruit two days after harvest; BC, AC - ‘Bartlett’ and ‘D’ Anjou’ fruit at 100% conditioning timepoint; BNC, ANC - ‘Bartlett’ and ‘D’ Anjou’ Non-Conditioned control fruit corresponding to 100% conditioning timepoint for fruit that received conditioning; BR, AR - ‘Bartlett’ and ‘D’ Anjou’ fruit at 100% Ripened stage; BNR, ANR - ‘Bartlett’ and ‘D’ Anjou’ Non-Conditioned control fruit corresponding to 100% ripening timepoint for fruit that received conditioning.





1162  
1163 **Figure 4.** Ray biplot representation of NMDS axis 1 and axis 2 (correlating to cultivar and phenology on  
1164 the x-axis and y-axis, respectively) contributions to expression variability between select gene targets  
1165 from final NMDS ordination. Dashed lines represent vector associated with genes in ordination space.  
1166 Image recreated from raw NMDS output in R. Quadrant shading added to highlight vector separation and  
1167 is not correlated to, or suggestive of, any physiological state. \*-indicates 'low confidence' values, defined  
1168 as those from which mean Ct equaled or exceeded 35.00, or whose efficiency exceeded 1.80-2.20 in at  
1169 least one replicate reactions. Raw R output available in Supplementary file 9.  
1170



1171  
 1172 **Figure 5.** Fold-change gene expression values (from -3 to +3) of topmost variably expressed genes from  
 1173 the qRT-PCR analysis in D'Anjou (columns 1-5), and Bartlett (columns 6-10), following sorting from  
 1174 final NMDS ordination. Grey cells indicate that a gene was not detected in the sample. \*-indicates 'low  
 1175 confidence' values, defined as those from which mean Cq equaled or exceeded 35.00, or whose efficiency  
 1176 exceeded 1.80-2.20 in at least one replicate reactions. Gene annotations on right side of the heatmap,  
 1177 labeled as letters A-G. A- cold signaling, B- transcriptional regulators, C- ethylene signaling, D- auxin  
 1178 signaling, E- abscisic acid signaling, F- peroxisomal or mitochondrial metabolite transport and  
 1179 respiration-related, G- internal controls. BH and AH – 'Bartlett' and 'D' Anjou' fruit two days after  
 1180 harvest; BC, AC - 'Bartlett' and 'D' Anjou fruit at 100% conditioning timepoint; 'BNC, ANC - 'Bartlett'  
 1181 and 'D' Anjou' Non- Conditioned control fruit corresponding to 100% conditioning timepoint for fruit  
 1182 that received conditioning; BR, AR - 'Bartlett' and 'D' Anjou' fruit at 100% Ripened stage; BNR, ANR -



1183 'Bartlett' and 'D'Anjou' Non-Conditioned control fruit corresponding to 100% ripening timepoint for  
1184 fruit that received conditioning. Heatmap generated with Morpheus with additional sample and pathways  
1185 annotated using Microsoft Powerpoint. Raw Morpheus output is available in Supplementary file 13.